



Accepted Article

Title: Indenyl compounds with constrained hapticity: the effect of strong intramolecular coordination.

Authors: Ondrej Mrozek; Jaromir Vinklarek; Zdenka Ruzickova; Jan Honzicek

This manuscript has been accepted after peer review and the authors have elected to post their Accepted Article online prior to editing, proofing, and formal publication of the final Version of Record (VoR). This work is currently citable by using the Digital Object Identifier (DOI) given below. The VoR will be published online in Early View as soon as possible and may be different to this Accepted Article as a result of editing. Readers should obtain the VoR from the journal website shown below when it is published to ensure accuracy of information. The authors are responsible for the content of this Accepted Article.

To be cited as: Eur. J. Inorg. Chem. 10.1002/ejic.201601029

Link to VoR: <http://dx.doi.org/10.1002/ejic.201601029>

Indenyl compounds with constrained hapticity: the effect of strong intramolecular coordination.

Ondřej Mrázek,^[a] Jaromír Vinklár, ^[a] Zdeňka Růžičková,^[a] and Jan Honzík*^[b]

Abstract: A series of cyclopentadienyl and indenyl molybdenum(II) compounds with intramolecularly coordinated pyridine arm, including scorpionate-like species bearing two irreversibly coordinated arms on the indenyl core, was synthesized and characterized. All presented structural types were confirmed by X-ray diffraction analysis. Due to strong nucleophilicity of pyridine, the intramolecular interaction is considerably stronger than in case of analogous species bearing tertiary amines in the side chain. Although the starting compounds for syntheses are isostructural, the reaction outcomes differ considerably. The cyclopentadienyl precursor gives a pentacoordinated η^5 : κN -compound while the indenyl analogue produces a hexacoordinated species with unprecedented η^3 : κN -coordination mode of the indenyl ligand representing an unusual example of so-called indenyl effect. The unusually high stability of the η^3 : κN -coordination compounds toward η^3 to η^5 haptotropic rearrangement was clarified by theoretical calculations. As the strong intramolecular interaction prevents rotation of the indenyl, it cannot reach the conformation suitable for the η^3 to η^5 rearrangement. As the result, the low hapticity is effectively locked.

Introduction

Cyclopentadienyl compounds of the transition metals attract considerable attention since ferrocene, $(\eta^5\text{-Cp})_2\text{Fe}$ (Cp = C₅H₅), was discovered in early 1950's.^[1] In the last decade, an increasing number of new ring-substituted cyclopentadienyl compounds has appeared in literature.^[2] The variations in the cyclopentadienyl ligand periphery often result in dramatic changes in physical, chemical and biological properties of the corresponding compounds.^[3] These changes can be, in particular cases, attributed to electronic and steric effects caused by the partial or full replacement of the hydrogen atoms by other groups.^[4]

A formal replacement of the cyclopentadienyl ligand with indenyl, a congener with annulated benzene ring (Ind = C₉H₇), usually accelerates rates of the substitution reactions due to a lower

energetic barrier of the haptotropic shift of the π -ligand. This so-called "indenyl effect" has been initially attributed to enhanced stability of the η^3 -intermediates in associative pathway as a consequence of the aromatic gain of the adjacent the six-membered ring.^[5] Although this approach is sometimes still accepted, it neglects different thermodynamic stability of the η^5 -Cp and η^5 -Ind species that may play a crucial role in the rearrangement as revealed by Veiros *et al.*^[6] They have demonstrated that the acceleration of the associative substitution reactions is a direct consequence of the different bonding of the ligands to metal in the η^5 and η^3 coordination modes. Hence, the $(\eta^5\text{-Cp})\text{-M}$ bond is considerably stronger than the $(\eta^5\text{-Ind})\text{-M}$ while the $(\eta^3\text{-Cp})\text{-M}$ is weaker than the $(\eta^3\text{-Ind})\text{-M}$ bond. This is reflected in the higher stability of η^5 -Cp complexes and the η^3 -Ind intermediates or transition states proving both a thermodynamic and a kinetic origin of the "indenyl effect" in associative reactions.

Some other mechanisms of the indenyl effect have been proposed for dissociative processes that are naturally not consistent with the η^5 - η^3 rearrangement. The electron deficient intermediate could be stabilized by interaction with the six-membered ring.^[7] Although the nature of the intermediate was not fully clarified, the indenyl ligand could achieve the η^9 -coordination mode that was documented later on low valent zirconium species.^[8] When dissociative substitution reaction involves the "spin forbidden" mechanism, the acceleration could be attributed to a lower barrier of the spin crossover as recently evidenced on iron(II) compounds.^[9]

The molybdenum(II) compounds were found to be very suitable for the investigation of the η^5 - η^3 rearrangements due to pronounced stability of the η^3 -indenyl species. Hence, they are often accessible from the η^5 -species by simple association of 2e donor into the coordination sphere of molybdenum(II) ^[10-13] or 2e reduction of molybdenum(IV) compounds.^[14]

The aim of the present work is to demonstrate the effect of annulated benzene ring on reactivity of cyclopentadienyl molybdenum compounds bearing strong *N*-donor in the side chain. The unprecedented structural motif consisting of the η^3 -indenyl species with the strong intramolecular coordination does NOT undergo the usual η^3 - η^5 rearrangement due to the kinetic stabilization as evidenced by combined experimental/theoretical study. To best of our knowledge, this is the first example of "locking" the species in η^3 -coordination mode by the intramolecular coordination.

Results and Discussion

Synthesis of allyl molybdenum precursors

The starting (2-pyridyl)methyl-substituted congeners of $[(\eta^3\text{-C}_3\text{H}_5)(\eta^5\text{-Cp})\text{Mo}(\text{CO})_2]$ (Cp' = Cp, Ind) were prepared using a

[a] O. Mrázek, J. Vinklár, Z. Růžičková
Department of General and Inorganic Chemistry,
Faculty of Chemical Technology, University of Pardubice
Studentská 573, 532 10 Pardubice, Czech Republic

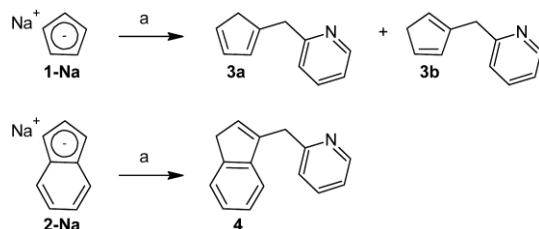
[b] J. Honzík
Institute of Chemistry and Technology of Macromolecular Materials
Faculty of Chemical Technology, University of Pardubice
Studentská 573, 532 10 Pardubice, Czech Republic
E-mail: jan.honzik@upce.cz

Supporting information for this article is given via a link at the end of the document.

FULL PAPER

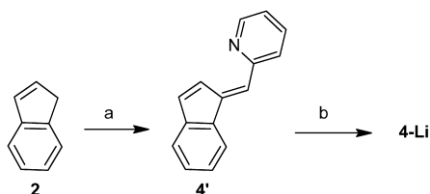
WILEY-VCH

general procedure developed by Faller *et al.*^[15] Functionalized cyclopentadiene $C_5H_4NCH_2C_5H_5$ (**3**) and indene 3- $(C_5H_4NCH_2)C_9H_7$ (**4**), necessary for the assembly, were synthesized using reaction of freshly distilled 2-(chloromethyl)pyridine with sodium cyclopentadienide (**1-Na**) and sodium indenide (**2-Na**), respectively (Scheme 1).



Scheme 1. Synthesis of the functionalized cyclopentadiene **3** and indene **4**. Reagents: a) $C_5H_4NCH_2Cl/THF$.

The alternative route is available for the indenide **4-Li**. It is given by hydrolithiation reaction of benzofulvene **4'** using Super-Hydride (Scheme 2). The starting **4'** was prepared in medium yield by condensation of indene (**2**) with 2-pyridinecarboxaldehyde. The 1H and $^{13}C\{^1H\}$ NMR measurements revealed appearance of the less steric hindered *E*-isomer only. This assignment was confirmed by X-ray diffraction analysis; see Figure 1. The molecule **4'** has almost planar structure. The dihedral angle between plane of the benzofulvene moiety and the pyridine ring is $3.72(5)^\circ$.

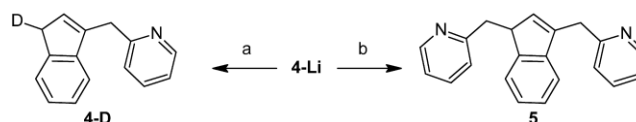


Scheme 2. Synthesis of the compound **4-Li** via fulvene intermediate. Reagents: a) C_5H_4NCHO , $MeONa/MeOH$; b) $Li[Et_3BH]/Et_2O$.

The indene **4** was further used for the synthesis of isotopically substituted derivative 1-D-3- $(C_5H_4NCH_2)C_9H_6$ (**4-D**) and 1,3-disubstituted indene 1,3- $(C_5H_4NCH_2)_2C_9H_6$ (**5**), see Scheme 3. 1H and $^{13}C\{^1H\}$ NMR spectroscopic measurements reveal that the compound **3** forms a mixture of isomers. At room temperature, 1- and 2-isomer appear in molar ratio 1.2 : 1. In case of the compound **4**, only one isomer was detected after the distillation purification step. The analytically pure sample of 1,3-disubstituted indene **5** was obtained after chromatographic purification step. The obtained sample was not contaminated with 1,1-isomer (expected byproduct) as evidenced by NMR measurements but its appearance in the crude product is not fully disputed. In the case of **4-D**, efficiency of the labeling was verified by the 1H NMR spectroscopy. The spectrum reveals that one hydrogen atom on sp^3 carbon of indene framework is fully substituted with deuterium.

Lithium cyclopentadienide **3-Li**, prepared by deprotonation of the cyclopentadiene **3** with *n*-BuLi, reacts with chloride complex $[(\eta^3-C_3H_5)Mo(CO)_2(NCMe)_2Cl]$ (**6**) to give the cyclopentadienyl

complex $[(\eta^3-C_3H_5)(\eta^5-C_5H_4NCH_2C_5H_4)Mo(CO)_2]$ (**7**), see Scheme 4. The indenyl complexes $[(\eta^3-C_3H_5)(\eta^5-1-(C_5H_4NCH_2)C_9H_6)Mo(CO)_2]$ (**8**), $[(\eta^3-C_3H_5)(\eta^5-1,3-(C_5H_4NCH_2)_2C_9H_5)Mo(CO)_2]$ (**9**) and isotopically labeled species $[(\eta^3-C_3H_5)(\eta^5-1-(C_5H_4NCH_2)-3-[D]C_9H_5)Mo(CO)_2]$ (**8-[D]**) were prepared accordingly starting from the indenenes **4**, **5**, and **4-D**, respectively.



Scheme 3. Synthesis of the functionalized indenenes **4-D** and **5**. Reagents: a) D_2O/THF ; b) $C_5H_4NCH_2Cl/THF$.

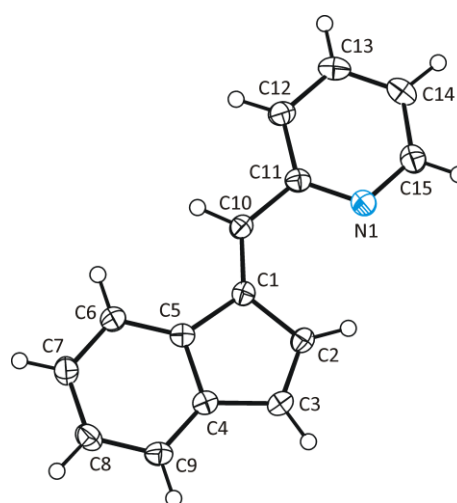
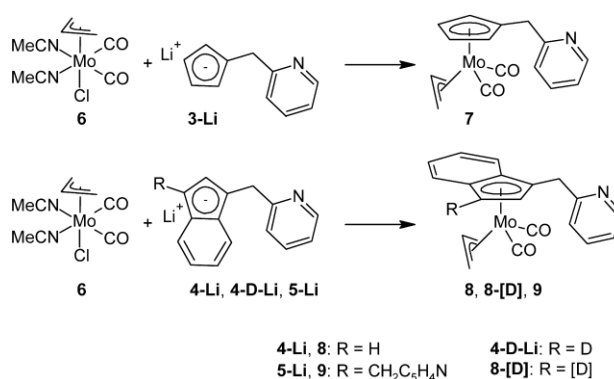


Figure 1. ORTEP drawing of the benzofulvene **4'**. The labeling scheme for all non-hydrogen atoms is shown. Thermal ellipsoids are drawn at the 50% probability level.



Scheme 4. Synthesis of the molybdenum compounds **7-9** and **8-[D]**.

Infrared spectrum of the cyclopentadienyl molybdenum compound **7** shows two CO stretching bands at 1927 and 1838 cm^{-1} . Higher wavenumbers observed for the indenyl derivatives **8** and **9** (~ 1933 and ~ 1854 cm^{-1}) reflect a lower electron density on the central metal that is caused by weaker donor properties of the indenyl ligand. Raman spectrum, measured for the

FULL PAPER

WILEY-VCH

derivative **9**, verifies the assignment of the band at lower frequency to the symmetric vibration mode (ν_s) as evident from considerably higher intensity. ^1H NMR spectra of the compounds **7–9** reveals a presence of two conformers arising from two distinct orientations of the allyl ligand. This behavior is in line with counterparts bearing unsubstituted cyclopentadienyl and indenyl ligands.^[15] The deuterium substituted indene **4-D** was used for synthesis of molybdenum compound selectively labeled in the 3-position of the indenyl ligand **8-D**. High efficiency of the labeling (65%) is due to kinetic isotope effect [$k(\text{H})/k(\text{D})$].

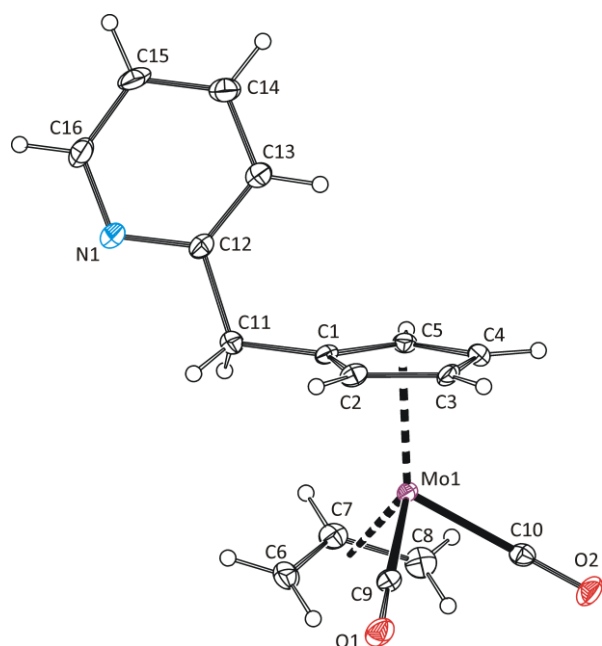


Figure 2. ORTEP drawing of the molecule $[(\eta^3\text{-C}_3\text{H}_5)(\eta^5\text{-C}_5\text{H}_4\text{NCH}_2\text{C}_5\text{H}_4)\text{Mo}(\text{CO})_2]$ present in the crystal structure of **7**. The labeling scheme for all non-hydrogen atoms is shown. Thermal ellipsoids are drawn at the 30% probability level. Only one of two crystallographically independent molecules is shown for clarity.

Table 1. Geometric parameters of the tetracoordinated molybdenum complexes.^[a]

	7 ^[b]	9
Mo–Cg(C ₅) ^[c]	2.014(3)	2.027(2)
Mo–Cg(C ₃) ^[c]	2.043(6)	2.048(3)
Mo–C(CO)	1.966(6) 1.941(4)	1.938(3) 1.936(3)
C(CO)–Mo–C(CO)	78.7(2)	80.0(2)
Cg(C ₅)–Mo–Cg(C ₃) ^[c]	127.0(4)	126.9(1)

[a] Distances are given in Å; angles are given in °. [b] Only data for one of two crystallographically independent molecules in the unit cell are given. [c] Cg is center of gravity.

Structures of the molybdenum compounds **7** and **9** were determined by the X-ray diffraction analysis. The molecules have a distorted tetrahedral structure with two carbonyl ligand, η^3 -allyl and the η^5 -coordinated π -ligand around molybdenum in the formal oxidation state II. In accordance with 18-electron rule the pendant arms are not coordinated.^[16]

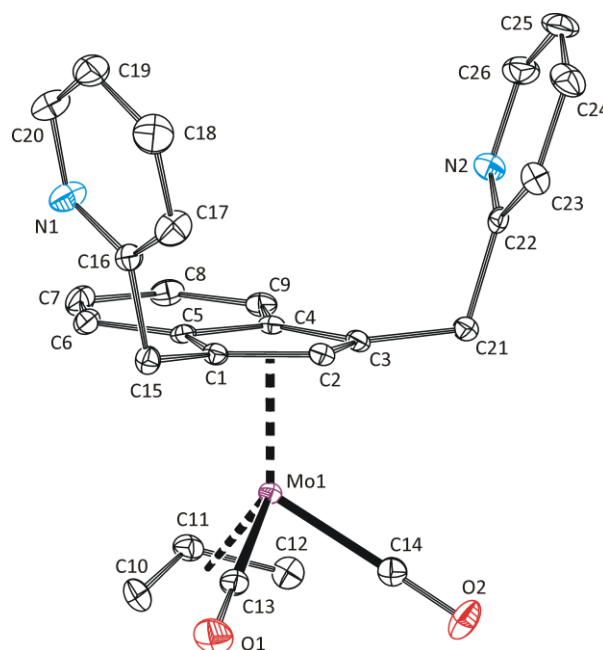
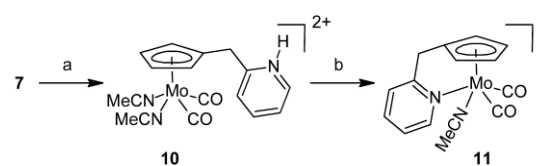


Figure 3. ORTEP drawing of the molecule $[(\eta^3\text{-C}_3\text{H}_5)(\eta^5\text{-1,3-C}_5\text{H}_4\text{NCH}_2\text{C}_5\text{H}_3)\text{Mo}(\text{CO})_2]$ present in crystal structure of **9**. The labeling scheme for all non-hydrogen atoms is shown. Thermal ellipsoids are drawn at the 30% probability level. Hydrogen atoms are omitted for clarity.

Cyclopentadienyl molybdenum compounds with intramolecular coordination

Reaction of the cyclopentadienyl molybdenum compound **7** with $\text{HBF}_4 \cdot \text{Et}_2\text{O}$ in presence of acetonitrile gives dicationic complex **10** with protonated pyridine arm. In acetone solution, this compound undergoes slow deprotonation that is accompanied by the exchange of MeCN ligand with pyridine of the side chain, see Scheme 5. The appeared compound with intramolecularly bonded pyridine arm (**11**) is inert toward strong acids in presence of coordinating solvents (e.g. $\text{HBF}_4 \cdot \text{Et}_2\text{O}/\text{MeCN}$) that demonstrates a high stability of $(\eta^5\text{-}k\text{N-C}_5\text{H}_4\text{NCH}_2\text{C}_5\text{H}_4)\text{Mo}^{\text{II}}$ moiety. Putative intermediate of the deprotonation reaction, $[(\eta^5\text{-C}_5\text{H}_4\text{NCH}_2\text{C}_5\text{H}_4)\text{Mo}(\text{CO})_2(\text{NCMe})_2][\text{BF}_4]$, was not observed probably due to fast coordination of pyridine arm that is driven by its strong nucleophilicity and the chelating effect.



Scheme 5. Reactivity of the cyclopentadienyl compound **7**. Reagents: a) $\text{HBF}_4 \cdot \text{Et}_2\text{O}$ (2 eq.)/MeCN, b) acetone.

FULL PAPER

WILEY-VCH

Infrared and Raman spectra of the compounds **10** and **11** show two CO stretching bands at higher wavelengths than observed for the allyl precursor **7** that is in line with a lower electron density on central metal. The intramolecular coordination of pyridine was easily recognized by ^1H NMR spectroscopy since the compound **10** is C_s symmetric while the species with coordinated pyridine arm **11** belongs to the point group C_1 . This decrease of the molecular symmetry is distinct mainly on the pattern of signals assigned to methylene bridge and the cyclopentadienyl ring. Hence, magnetically equivalent protons of CH_2 group in **10** give one singlet at 4.10 ppm while AB quartet ($\Delta\delta_{\text{AB}} = 0.09$ ppm, $^2J = 19.8$ Hz) at 4.39 ppm was observed for the compound **11**. Furthermore, the C_s -symmetric species **10** gives two pseudo-triplets (AA'BB' spin system) at 5.66 and 5.96 ppm for four protons of the cyclopentadienyl ring while the lower symmetric compound **11** show four multiplets (ABCD spin system) at 5.19–6.65 ppm.

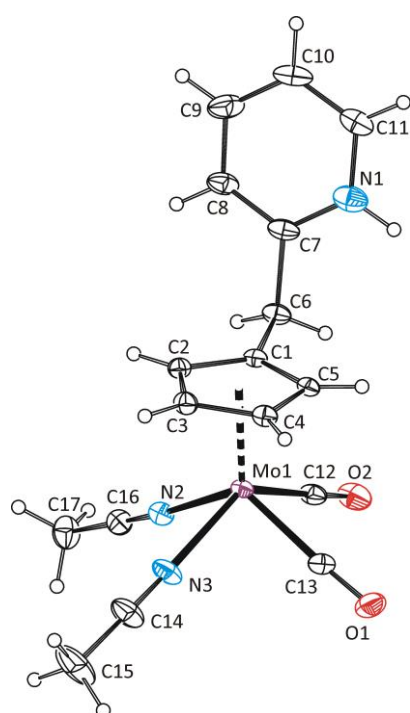


Figure 4. ORTEP drawing of the dication $[(\eta^5\text{-C}_5\text{H}_4\text{NHCH}_2\text{C}_5\text{H}_4)\text{Mo}(\text{CO})_2(\text{NCMe})_2]^{2+}$ present in crystal structure of **10**. The labeling scheme for all non-hydrogen atoms is shown. Thermal ellipsoids are drawn at the 30% probability level.

The crystal structures of the compounds **10** and **11** were determined by X-ray diffraction analysis (Figs 4 and 5). Both compounds have a distorted square-pyramidal structure with the η^5 -bonded cyclopentadienyl ligand in the apical position and two carbonyls in adjacent vertices of the basal plane. In the species **10**, two acetonitrile ligands occupy remaining vertices of the basal plane. In the case of **11**, these two positions are occupied with one acetonitrile ligand and the intramolecularly bonded pyridine. Bond distance Mo–N [2.229(4)–2.238(4) Å] is considerably shorter than reported for species bearing intramolecularly coordinated tertiary amine $[(\eta^5\text{-}\kappa\text{N-Me}_2\text{NCH}_2\text{CH}_2\text{C}_5\text{H}_4)\text{Mo}(\text{CO})_2]$ [(2.380(3) Å)]^[17] but comparable

with more nucleophilic primary amine $[(\eta^5\text{-}\kappa\text{N-H}_2\text{NCH}_2\text{CH}_2\text{C}_5\text{H}_4)\text{Mo}(\text{CO})_2(\text{PPh}_3)][\text{PF}_6]$ [2.254(8) Å].^[18]

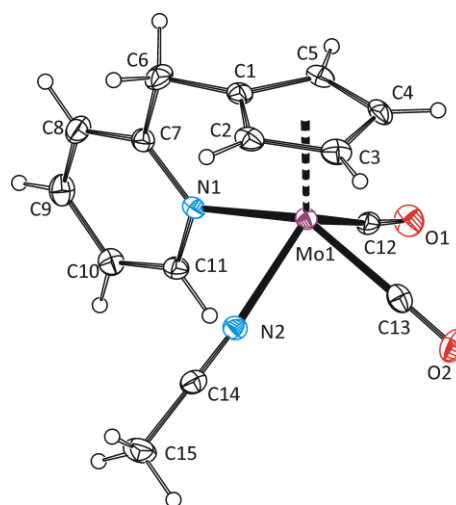


Figure 5. ORTEP drawing of the cation $[(\eta^5\text{-}\kappa\text{N-C}_5\text{H}_4\text{NCH}_2\text{C}_5\text{H}_4)\text{Mo}(\text{CO})_2(\text{NCMe})]^{+}$ present in crystal structure of **11**. The labeling scheme for all non-hydrogen atoms is shown. Thermal ellipsoids are drawn at the 30% probability level. Only one of three crystallographically independent molecules is shown for clarity.

Table 2. Geometric parameters of the pentacoordinated molybdenum complexes.^[a]

	10	11 ^[b]	12	13
Mo–Cg(C_5) ^[a]	1.980(1)	1.964(1)	1.985(3)	1.9767(3)
Mo–C(CO)	1.981(4) 1.966(3)	1.999(4) 1.942(4)	2.028(4) 1.928(4)	1.942(2) 1.993(2)
Mo–N1	–	2.229(4)	2.256(3)	2.237(2)
Mo–X ^[c]	2.165(3) 2.167(3)	2.156(3)	2.230(3)	2.4910(4)
C(CO)–Mo–C(CO)	74.6(2)	76.3(2)	78.8(2)	77.3(1)
X–Mo–N ^[c]	78.4(2)	77.9(2)	78.8(1)	78.85(4)
α ^[d]	–	0.3(3)	1.1(3)	8.3(2)
β ^[e]	–	10.2(5)	1.2(4)	0.8(2)

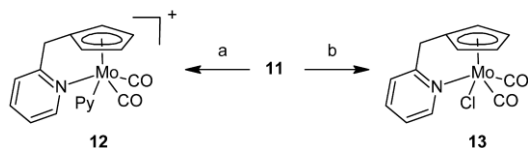
[a] For units or definition see footnote of the Table 1. [b] Only data for one of three crystallographically independent molecules in the unit cell are given. [c] **10**: X = N2, N3; **11**, **12**: X = N2; **13**: X = C11. [d] α represents orientation of the pyridine toward axis defined by Mo–Cg(C5). It is defined as absolute value of dihedral angle Cg(C5)–Mo1–N1–C7. [e] β represents twisting of the coordinated arm. It is defined as absolute value of dihedral angle C1–C6–C7–N1.

The acetonitrile ligand of the compound **11** could be easily exchanged by 2e-ligands such as pyridine or chloride, see Scheme 6. ^1H NMR spectra of the products **12** and **13** show a pattern consistent with the C_1 molecular symmetry. Methylene

FULL PAPER

WILEY-VCH

groups of the intramolecular bridge give AB quartets (**12**: $\delta = 4.55$ ppm, $\Delta\delta_{AB} = 0.30$ ppm, $^2J = 19.8$ Hz; **13**: $\delta = 4.26$ ppm, $\Delta\delta_{AB} = 0.06$ ppm, $^2J = 19.8$ Hz) that is typical for the rigid low-symmetric compounds. Protons of the cyclopentadienyl ring appear as four multiplets of the ABCD spin system.



Scheme 6. Reactivity of the cyclopentadienyl compound **11**. Reagents: a) Py/CH₂Cl₂, b) [Me₄N]Cl/acetone.

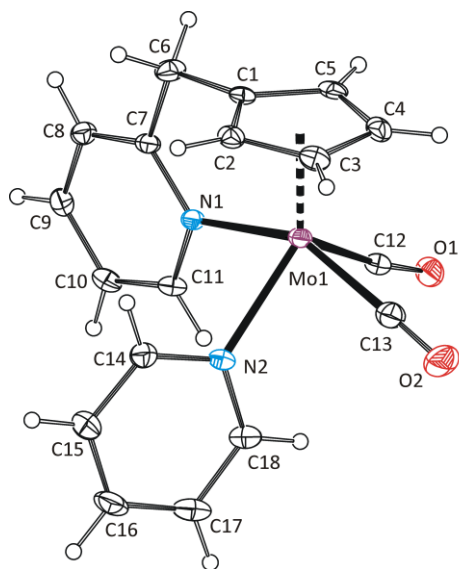


Figure 6. ORTEP drawing of the cation [(η^5 - κN -C₅H₄NCH₂C₅H₄)Mo(CO)₂(py)]⁺ present in crystal structure of **12**. The labeling scheme for all non-hydrogen atoms is shown. Thermal ellipsoids are drawn at the 30% probability level.

Infrared and Raman spectra of the neutral chloride complex **13** show the CO stretching bands at considerably lower wavenumbers than the cationic analogues bearing acetonitrile (**11**) or pyridine ligand (**12**). This is due to higher electron density on the metal that enhances the back donation into π^* -orbitals of carbonyl ligands.

The structures of **12** and **13**, elucidated by analytical and spectroscopic measurements, were further verified by the X-ray diffraction analysis (Figs. 6 and 7). In the case of **12**, the bond distance between molybdenum atom and nitrogen of the pyridine ligand [Mo–N2 = 2.230(3) Å] is very similar to the intramolecularly coordinated pyridine arm [Mo–N2 = 2.256(3) Å]. Evidently, the chelate effect on the bond distance Mo–N1 is here compensated with weaker *trans* effect of the carbonyl ligands [N1–Mo–C13 = 150.1(2)°, N2–Mo–C12 = 104.9(2)°].

The compounds **12** and **13** are inert toward excess of pyridine and [Me₄N]Cl, respectively. It suggests considerably stronger intramolecular interaction than recently reported for analogues with tertiary amines connected to the cyclopentadienyl ring via ethylene bridge.^[19] Due to strong nucleophilicity of pyridine, the (η^5 - κN -C₅H₄NCH₂C₅H₄)Mo^{II} moiety in **11** is not disrupted even by

the strong *N,N*-chelators (e.g. bpy, phen). We note that the tertiary amine-functionalized analogues give under similar conditions solely species without the intramolecular interaction [(η^5 -R₂NCH₂CH₂C₅H₄)Mo(CO)₂(phen)][BF₄].^[19]

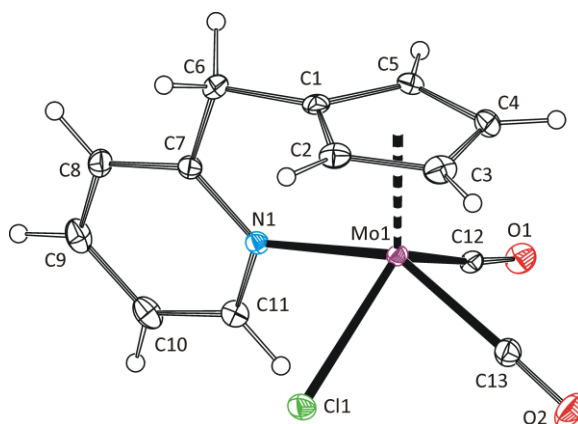
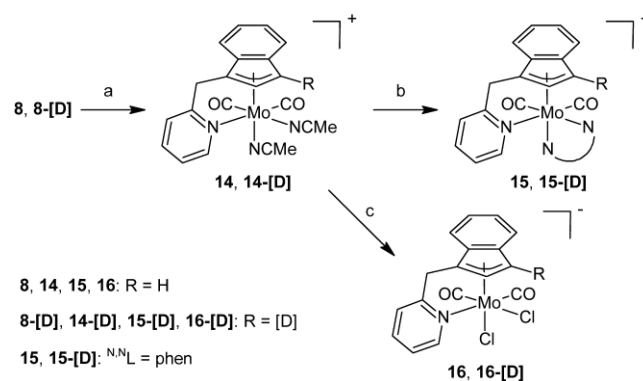


Figure 7. ORTEP drawing of the molecule [(η^5 - κN -C₅H₄NCH₂C₅H₄)Mo(CO)₂Cl] present in crystal structure of **13**. The labeling scheme for all non-hydrogen atoms is shown. Thermal ellipsoids are drawn at the 30% probability level.

Indenyl molybdenum compounds with intramolecular coordination

Reaction of the indenyl molybdenum compound **8** with HBF₄·Et₂O in presence of acetonitrile leads, similarly as in case of the cyclopentadienyl analogue **7**, to the protonation of η^3 -allyl ligand and consequent coordination of acetonitrile ligands. Surprisingly, the standard work up does not give the expected pentacoordinated species with the η^5 -bonded indenyl but solely hexacoordinated η^3 -indenyl complex with the intramolecularly coordinated pyridine arm (**14**), see Scheme 7.



Scheme 7. Reactivity of the indenyl compounds **8** and **8-[D]**. Reagents: a) HBF₄·Et₂O (1 eq.), MeCN (2 eq.)/CH₂Cl₂, b) phen/MeCN, c) [Me₄N]Cl/acetone.

Infrared spectrum of the compound **14** shows two bands in the range typical for terminal carbonyl ligands. The hapticity of the indenyl ligand was elucidated from the ¹H NMR measurements. According to previous studies on various indenyl compounds without substituents in the five-membered ring,^[10, 12, 13] the chemical shifts of H^{1/3} and H² are diagnostic for the hapticity elucidation. Hence, in case of organometallic compounds bearing the η^3 -indenyl ligand, the signal of H² appears at

FULL PAPER

WILEY-VCH

considerably lower field than $H^{1/3}$ while the η^5 -species have the signal of H^2 at higher field. This relation is, of course, applicable on our species bearing a substituent in 1-position but only after the unambiguous assignment of two doublets ($^2J = 3.9$ Hz) to the protons H^2 and H^3 . It led us to use the deuterium labeled derivative **8-D** for synthesis of **14-D** (Scheme 7). The labeling results in considerable decrease of the doublet at 5.14 ppm (H^3) in intensity and in broadening of signal at 6.83 ppm (H^2) due to spin-spin interactions H^2 -[D] 3 . This experiment unambiguously revealed the η^3 -coordination mode of the indenyl ligand that was further confirmed in solid state by the X-ray diffraction analysis (Fig. 8).

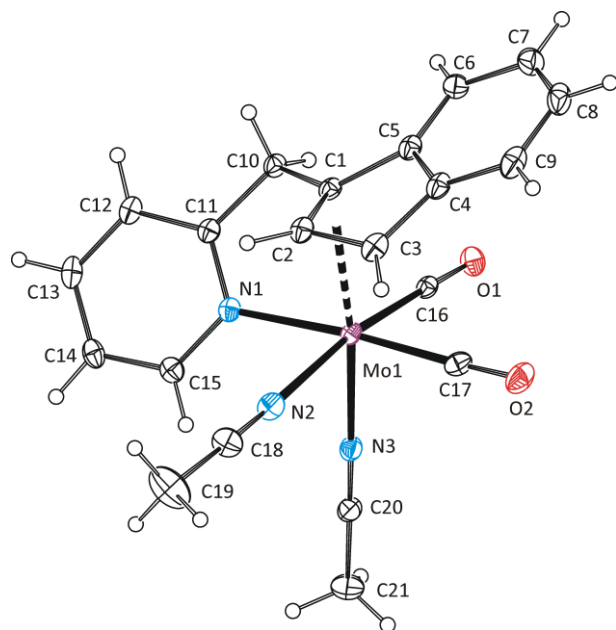


Figure 8. ORTEP drawing of the cation $[(\eta^3:\kappa N-1-(C_5H_4NCH_2)C_9H_6)Mo(CO)_2(NCMe)_2]^+$ present in crystal structure of **14**·CH₂Cl₂. The labeling scheme for all non-hydrogen atoms is shown. Thermal ellipsoids are drawn at the 30% probability level.

The exchange of acetonitrile ligands does not disrupt the coordination of pyridine arm as demonstrated on reactions with 1,10-phenanthroline and [Me₄N]Cl, see Scheme 7. In both cases, only products of simple ligand exchange were isolated. The retention of indenyl ligand hapticity in the species **15** and **16** was confirmed by the deuterium labeling study. Similarly as observed for the compound **14**, signal of the indenyl proton H^2 appears in the ¹H NMR spectra at considerably lower field than the signal of H^3 .

Although the appearance of dichloride **16** seems to be obvious, this is rather unusual. From the mechanistic point of view, one may expect formation of pentacoordinated species with coordination sphere resembling the recently described chloride complex $[(\eta^5-4,7-Me_2C_9H_5)Mo(CO)_2(py)Cl]$.^[12] The unusual stability of the compound **16** is probably not only a result of the constrained geometry but also due to the high energetic barrier of the η^3 : η^5 -indenyl ring slippage as will be discussed in detail later on the compound **14**.

Crystal structures of **14**, **15** and **16**·½Me₂CO were determined by the X-ray diffraction analysis (Figures 8–10). The molecules have a distorted octahedral structure with one face occupied by

centroid of the indenyl ligand and two carbonyl ligands. The opposite octahedral face is occupied by nitrogen atom of the pyridine arm and two donor atoms of remaining ligands. Due to short intramolecular bridge, the pyridine arm and the indenyl are in *cis*-configuration. High values of the envelop fold angle [$\Omega = 25.0(5)$ – $26.3(6)^\circ$] and $\Delta(M-C)$ [0.830(5)–0.871(4) Å], observed for the indenyl ligand, verifies the η^3 -coordination mode. The indenyl ligand takes a configuration with the C₆-ring above carbonyls that is common for the hexacoordinated molybdenum compounds without intramolecular coordination.^[12, 13, 20] The η^3 : κN -coordination mode of the functionalized indenyl ligand is unprecedented. Hence, the more conventional η^5 : κN is reported for number of lanthanide^[21] and group IV metal compounds.^[22] The species of intermediate hapticity between η^5 and $\eta^{2:1}$ was described on nickel complex $[(\eta^{5\leftrightarrow 2:1}:\kappa N-1-(C_5H_4NCH_2)C_9H_6)Ni(PPh_3)][BPh_4]$.^[23] This species has considerably lower values of the ring slip parameters Ω [11.48(14) $^\circ$] and $\Delta(M-C)$ [0.242(3) Å] than observed for η^3 : κN -molybdenum complexes reported here; see Table 3.

Table 3. Geometric parameters of the hexacoordinated molybdenum complexes.^[a]

	14	15	16 ^[b]	18
Mo–Cg(C ₃) ^[a]	2.069(4)	2.063(4)	2.078(4)	2.051(1)
Mo–C(CO)	2.002(4) 1.966(4)	1.978(4) 1.957(4)	1.960(5) 1.934(5)	1.979(2) 1.963(2)
Mo–N1	2.270(3)	2.274(3)	2.282(4)	2.284(2)
Mo–X _{eq} ^[c]	2.222(4)	2.259(3)	2.568(2)	2.302(2)
Mo–X _{ax} ^[d]	2.162(4)	2.200(4)	2.517(2)	2.167(2)
X _{ax} –Mo–Cg(C ₃) ^[a,d]	172.9(2)	171.6(2)	175.2(2)	171.7(1)
C(CO)–Mo–C(CO)	82.6(2)	82.0(2)	81.6(2)	80.6(1)
N1–Mo–X _{eq} ^[c]	83.7(2)	88.0(2)	87.0(1)	95.2(1)
Ω ^[e]	25.5(5)	26.3(4)	25.0(5)	26.9(3)
$\Delta(M-C)$ ^[f]	0.842(4)	0.871(4)	0.830(5)	0.842(3)
α ^[g]	34.2(3)	35.0(3)	35.3(3)	40.2(2) ^[i]
β ^[h]	31.2(5)	26.3(5)	26.6(5)	23.8(3) ^[i]

[a] For units or definition see footnote of the Table 1. [b] Only data for one of two crystallographically independent molecules in the unit cell are given. [c] **14**, **15**, **17**: X_{eq} = N2; **16**: X_{eq} = C11. [d] **14**, **15**, **17**: X_{ax} = N3; **16**: X_{ax} = C12. [e] Ω is the fold angle between planes defined by C1, C2, C3 and that of C1, C3, C4, C5.^[24] [f] $\Delta(M-C)$ represents the differences in the metal-carbon bonds. It is defined as the difference between the averages of the distances Mo–C4, Mo–C5 and those of Mo–C1, Mo–C2, Mo–C3.^[24] [g] α is defined as absolute value of dihedral angle Cg(C3)–Mo1–N1–C11; [h] β is defined as absolute value of dihedral angle C1–C10–C11–N1. [i] The values for the second coordinated arm are $\alpha = 35.3(2)^\circ$; $\beta = 25.5(3)^\circ$.

In contrast to the cyclopentadienyl compounds **11–13**, the indenyl complexes do not have the plane of pyridine ring parallel to the axis Cg–Mo and the arm is twisted as evident from considerably higher values of the parameters α [34.2(3)–38.0(3) $^\circ$] and β [19.6(6)–31.2(5) $^\circ$], respectively (*cf.* with data in

FULL PAPER

WILEY-VCH

Table 2). Furthermore, the intramolecular bond Mo–N1 is considerably longer than found in the cyclopentadienyl species **11–13**. The prolongation, observed for the indenyl compounds, is due to a more efficient *trans* effect of the carbonyl ligands. This phenomenon also clarifies the systematically longer bonds Mo–X_{eq} when compared to the Mo–X_{ax}, see Table 3.

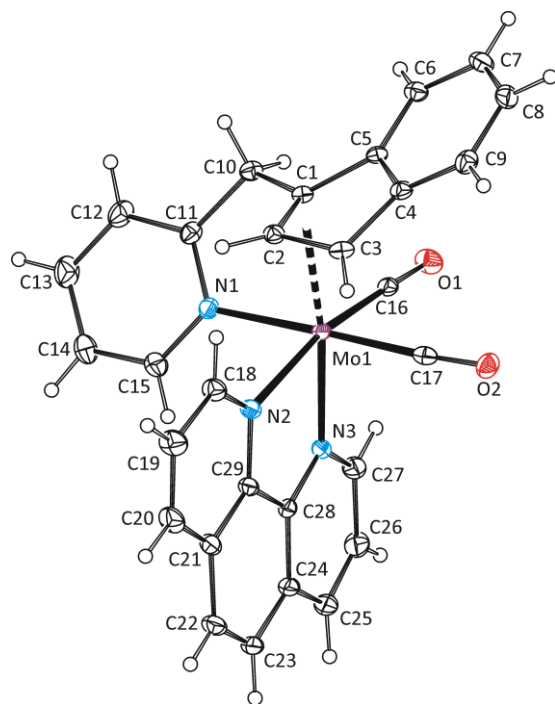


Figure 9. ORTEP drawing of the cation $[\{\eta^3\text{-}\kappa\text{N-1-(C}_5\text{H}_4\text{NCH}_2\text{)C}_9\text{H}_6\}\text{Mo(CO)}_2(\text{phen})\}]^+$ present in crystal structure of **15**. The labeling scheme for all non-hydrogen atoms is shown. Thermal ellipsoids are drawn at the 30% probability level.

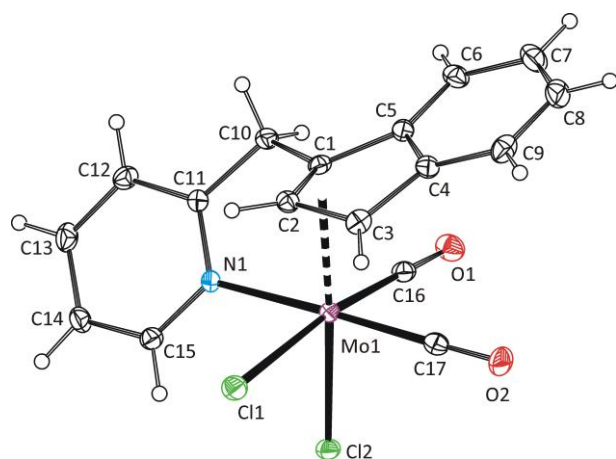
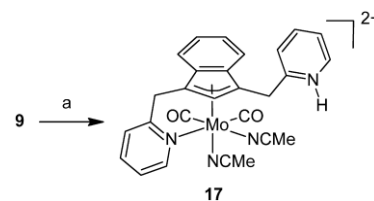


Figure 10. ORTEP drawing of the anion $[\{\eta^3\text{-}\kappa\text{N-1-(C}_5\text{H}_4\text{NCH}_2\text{)C}_9\text{H}_6\}\text{Mo(CO)}_2\text{Cl}_2\text{]}^-$ present in crystal structure of **16**. $1/2\text{Me}_2\text{CO}$. The labeling scheme for all non-hydrogen atoms is shown. Thermal ellipsoids are drawn at the 30% probability level. Only one of two crystallographically independent molecules is shown for clarity.

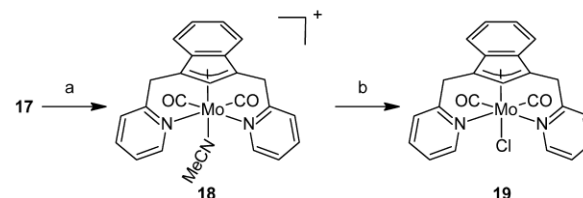
The indenyl complex bearing two pyridine arms **9** reacts with $\text{HBF}_4\cdot\text{Et}_2\text{O}$ to give dicationic species **17**, see Scheme 8. In this

compound, one pyridine arm is protonated while the second one is intramolecularly coordinated to the central metal. The indenyl ring is η^3 -bonded as evident from the low-fielded signal of H^2 ($\delta = 7.18$ ppm). The methylene group of the uncoordinated arm gives AB quartets with a very low value of $\Delta\delta_{\text{AB}}$ (0.04 ppm). A considerably higher separation appears in the coordinated arm ($\Delta\delta_{\text{AB}} = 0.28$ ppm), which is in line with observations on the structurally related complexes **14–16**.



Scheme 8. Reactivity of the indenyl compound **9**. Reagents: a) $\text{HBF}_4\cdot\text{Et}_2\text{O}$ (3 eq.)/MeCN.

The pyridinium ring in the side arm of **17** could be deprotonated by an excess of pyridine. This process is accompanied with exchange of the MeCN ligand (the one in *cis*-position to the indenyl) with pyridine of the side chain to give a novel scorpionate-like compound **18** bearing two irreversibly coordinated arms on the indenyl core. Due to steric hindrance, the second MeCN ligand (in *trans*-position to the indenyl) is not exchanged by the excess pyridine. Nevertheless, it could be exchanged by less demanding chloride ligand to give the compound **19**, see Scheme 9.



Scheme 9. Reactivity of the indenyl compound **17**. Reagents: a) py b) $[\text{Me}_4\text{N}]\text{Cl}/\text{acetone}$.

The compounds with two intramolecularly bonded pyridine arms (**18** and **19**) are C_s symmetric as evident from the pattern of ^1H NMR spectra. In both cases, the methylene groups give one AB quartet with $^2J \sim 19.5$ Hz (**18**: $\Delta\delta_{\text{AB}} = 0.27$ ppm, **19**: $\Delta\delta_{\text{AB}} = 0.39$ ppm). The indenyl proton H^2 appears at a low field (**18**: 6.38 ppm, **19**: 6.26 ppm) that is consistent with the η^3 -coordination mode. In the case of compound **18**, the proposed molecular structure was confirmed in solid state by the X-ray diffraction analysis, see Figure 11. The molecule has a distorted octahedral structure of approximate C_s symmetry. The tridentate indenyl ligand is coordinated symmetrically as revealed from similar bond lengths Mo–N, see Table 3. The η^3 -coordination mode of the indenyl is evidenced by high values of the ring slip parameters Ω [$26.9(3)^\circ$] and $\Delta(\text{M–C})$ [$0.842(3)$ Å].

FULL PAPER

WILEY-VCH

Since the opposite orientation of the indenyl ligand toward $\text{Mo}(\text{CO})_2$ moiety is observed for the species **A** and **D'**, the haptotropic rearrangement have to be accompanied with the 180° rotation of the indenyl ligand. The rotation barrier of the η^3 -bonded indenyl ligand is $9.3 \text{ kcal}\cdot\text{mol}^{-1}$. The conformer with the $\sim 90^\circ$ rotated indenyl (**B**) has an energy $5.9 \text{ kcal}\cdot\text{mol}^{-1}$ and the conformer **C** with 180° rotation (C_6 -ring *trans* to carbonyls) $7.8 \text{ kcal}\cdot\text{mol}^{-1}$. Rotation of the η^5 -bonded indenyl ligand in the pentacoordinated species **D'** is also kinetically allowed as evidenced by the low energy barrier of $8.5 \text{ kcal}\cdot\text{mol}^{-1}$. Transition states of the ring slippage step were calculated for all three pairs of conformers with the same orientation of the indenyl ligand (TS_{AF} , TS_{BE} and TS_{CD}). The lowest barrier ($16.9 \text{ kcal}\cdot\text{mol}^{-1}$) appears between the conformers **C** and **D** having the C_6 -ring of indenyl ligand *trans* to the carbonyl ligands. In appropriate transition state (TS_{CD}), the indenyl ring slips from η^3 to η^5 , as evidenced by the folding angle (Ω) of 15.6° , while dissociation of the $\text{Mo}-\text{N}_{\text{ax}}$ bond is underway with a distance of 2.93 \AA and a Wiberg index (WI) $^{[28]}$ of 0.23 , indicating a weak interaction. The pathways of the ring slippage starting from the conformers **A** and **B** are kinetically disfavored owing to considerably higher activation energies (TS_{AF} : $33.1 \text{ kcal}\cdot\text{mol}^{-1}$; TS_{BE} : $24.5 \text{ kcal}\cdot\text{mol}^{-1}$). Consequently, the preferred pathway comprises the 180° rotation of the η^3 -bonded indenyl ligand (**A** \rightarrow **B** \rightarrow **C**) followed with the η^3 to η^5 indenyl ring slippage accompanied with acetonitrile dissociation (**C** \rightarrow **D'**) that is a rate determining step.

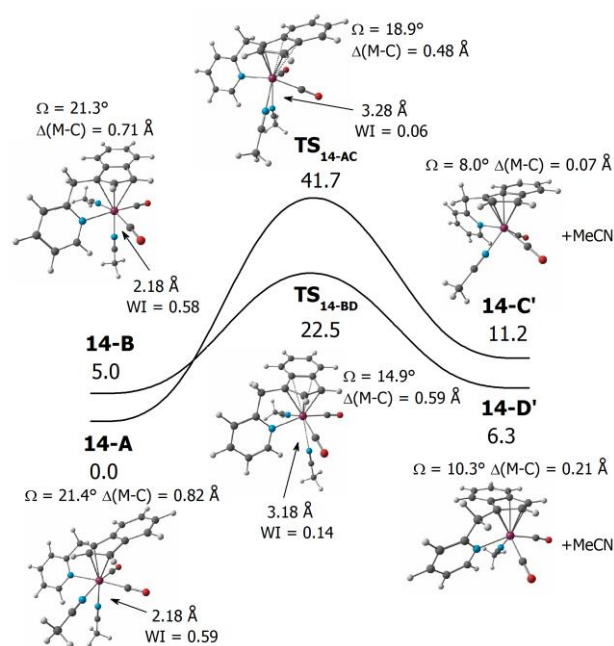


Figure 13. Energy profile (B3LYP) of the haptotropic rearrangement of indenyl ligand in the complex **14**. The energy is given in $\text{kcal}\cdot\text{mol}^{-1}$ and referred to the reagent **14-A**.

In the case of compound **14**, observed isomer, with the C_6 -ring of indenyl ligand above the carbonyls (**14-A**), is thermodynamically favored as confirmed by theoretical calculations. Hence, the virtual isomer with the C_6 -ring above $\text{Mo}(\text{CO})(\text{NCMe})$ moiety (**14-B**) is $5.0 \text{ kcal}\cdot\text{mol}^{-1}$ less stable ($\Delta G = 5.2 \text{ kcal}\cdot\text{mol}^{-1}$). We note that further suggested isomer with C_6 -ring *trans* to carbonyls is not an energetic minimum due to strain

of the coordinated pyridine arm. As rotation of the indenyl ligand is restricted by the strong intramolecular interaction, the observed species **14-A** could only rearrange to **14C'** while the thermodynamically favored product **14D'** is only available from the virtual isomer **14-B**, see Figure 13. The **14-A** \rightarrow **14C'** transition is not kinetically allowed due to high activation energy ($41.7 \text{ kcal}\cdot\text{mol}^{-1}$). In accordance to afore-mentioned system without intramolecular coordination, the η^3 to η^5 slippage is more convenient in the other orientations of the indenyl ligand. Hence, the **14-B** \rightarrow **14D'** transition shows considerably lower activation energy ($17.5 \text{ kcal}\cdot\text{mol}^{-1}$) and significant free energy gain ($\Delta G = -9.9 \text{ kcal}\cdot\text{mol}^{-1}$). As the isomer for the kinetically allowed pathway (**14-B**) is not available in the reaction mixture, the η^3 to η^5 cannot proceed under mild conditions.

Conclusions

In conclusion, we have demonstrated an unusual example of the indenyl effect on the cyclopentadienyl and indenyl molybdenum compounds with pyridine in the side chain (**7** and **8**). Although the species are isostructural, their reactivity differs considerably. The cyclopentadienyl compound **7** produces rather convenient pentacoordinated η^5 : κN -species **11** while the hexacoordinated species with unprecedented η^3 : κN -coordination mode **14** was synthesized from the indenyl analogue **8** under similar reaction conditions. Further experiments, performed on both reaction products, have confirmed irreversible character of the intramolecular coordination. The unusually high stability of the indenyl complex **14** toward the η^3 to η^5 haptotropic rearrangement was clarified by the theoretical calculations. Since strong intramolecular interaction prevents rotation of the indenyl ligand, it cannot achieve conformation suitable for the haptotropic rearrangement. Thus, the intramolecular coordination performs as a lock preserving the low hapticity of the indenyl ligand.

Experimental Section

Methods and materials. All operations were performed under nitrogen atmosphere using conventional Schlenk-line techniques. The solvents were purified and dried by standard methods.^[29] Starting materials were available commercially or prepared according to literature procedures: NaCp (**1**),^[30] NaInd (**2**),^[31] $[(\eta^3\text{-C}_3\text{H}_5)\text{Mo}(\text{CO})_2(\text{NCMe})_2\text{Cl}]$ (**6**).^[15]

Measurements. Infrared and Raman spectra were recorded on a Nicolet iS50 FTIR spectrometer equipped a Raman module (Nd:YAG laser emitting at 1064 cm^{-1}). The infrared spectra were recorded in the $4000\text{--}400 \text{ cm}^{-1}$ region (resolution 1 cm^{-1}) using Diamond Smart Orbit ATR. Raman spectra were recorded in the $4000\text{--}100 \text{ cm}^{-1}$ region (resolution 2 cm^{-1}) in glass capillaries. The ^1H and $^{13}\text{C}\{^1\text{H}\}$ NMR spectra were recorded on a Bruker Avance 400 and Bruker Avance 500 spectrometers at 300 K in CDCl_3 , CD_3CN , acetone- d_6 and $\text{DMSO-}d_6$. The chemical shifts are given in ppm relative to TMS. Mass spectrometry was performed on a quadrupole mass spectrometer (LCMS 2010, Shimadzu, Japan). The sample was injected into the mass spectrometer with infusion mode at a constant flow rate of $10 \mu\text{L}/\text{min}$. Electrospray ionization-mass spectrometry (ESI-MS) was used for the identification of analyzed samples.

Synthesis of $\text{C}_5\text{H}_4\text{NCH}_2\text{Cl}$. A solution of KOH (15 g , 0.27 mol) in distilled water (150 mL) was cooled to 0°C and treated with $\text{C}_5\text{H}_4\text{NCH}_2\text{Cl}\cdot\text{HCl}$

FULL PAPER

WILEY-VCH

(21.3 g, 0.13 mol). The reaction mixture was extracted with CH_2Cl_2 (4 × 50 mL) and combined organic layers were dried with magnesium sulfate. The volatiles were evaporated on rotavapor and the crude product was vacuum distilled at 74 °C (10 Torr). Yield: 14.9 g (0.12 mol, 90%). Colorless liquid. Analytical and spectroscopic data are in line with those published elsewhere.^[32]

Synthesis of $\text{C}_5\text{H}_4\text{NCH}_2\text{C}_5\text{H}_5$ (3). A solution of NaCp (1; 4.40 g, 50 mmol) in THF (150 mL) was cooled to 0 °C, treated with $\text{C}_5\text{H}_4\text{NCH}_2\text{Cl}$ (5.87 g, 46 mmol) dropwise and stirred at room temperature overnight. The reaction mixture was poured into distilled water (75 mL) and crude product was extracted with CH_2Cl_2 (4 × 50 mL). Combined organic layers were dried with magnesium sulfate. The volatiles were evaporated on rotavapor and the crude product was vacuum distilled using Kugelrohr apparatus (150 °C, 10 Torr). Yield: 4.55 g (29 mmol, 63%). Pale yellow liquid. Analytical and spectroscopic data are in line with those published elsewhere.^[33]

Synthesis of $3\text{-(C}_5\text{H}_4\text{NCH}_2\text{)}_2\text{C}_9\text{H}_7$ (4). The reaction was carried out as described for compound 3 but with NaInd (2; 6.91 g, 50 mmol). The crude product was vacuum distilled using Kugelrohr apparatus (300 °C, 6 Pa). Yield: 4.00 g (19 mmol, 42%). Orange liquid. Analytical and spectroscopic data are in line with those published elsewhere.^[33]

Synthesis of 1-D-3-($\text{C}_5\text{H}_4\text{NCH}_2$) C_9H_6 (4-D). A solution of 3-($\text{C}_5\text{H}_4\text{NCH}_2$) C_9H_7 (4; 5.18 g, 25 mmol) in THF (30 mL) was cooled to 0 °C, treated with a solution of $^n\text{BuLi}$ in hexane (15.6 mL, 1.6 mol/L, 25 mmol) dropwise and stirred for 30 min. at this temperature. The reaction mixture was treated with D_2O (3 mL, 165 mmol) dropwise, allowed to warm up to room temperature, slowly poured into distilled water (50 mL) and extracted with CH_2Cl_2 (4 × 50 mL). Combined organic layers were dried with magnesium sulfate. The volatiles were evaporated on rotavapor and the product was vacuum distilled using Kugelrohr apparatus (240 °C, 6 Pa). Yield: 4.4 g (21 mmol, 72%). Orange liquid. ^1H NMR (CDCl_3 , 400.13 MHz): δ = 3.44 (m, 1H, H^1 , C_9H_6), 4.20 (s, 2H, CH_2), 6.33 (m, 1H, H^2 , C_9H_6), 7.20 (ddd, $^3J(\text{H}^1, \text{H}^1) = 7.5$ Hz, $^3J(\text{H}^1, \text{H}^1) = 5.1$ Hz, $^4J(\text{H}^1, \text{H}^1) = 0.7$ Hz, 1H, $\text{H}^{4/5}$, $\text{C}_5\text{H}_4\text{N}$), 7.24–7.35 (m, 3H, H^{4-7} , C_9H_6), 7.39 (d, $^3J(\text{H}^1, \text{H}^1) = 7.6$ Hz, $\text{H}^{4/7}$, C_9H_6), 7.53 (d, $^3J(\text{H}^1, \text{H}^1) = 7.6$ Hz, $\text{H}^{3/6}$, $\text{C}_5\text{H}_4\text{N}$), 7.63 (td, $^3J(\text{H}^1, \text{H}^1) = 7.6$ Hz, $^4J(\text{H}^1, \text{H}^1) = 1.7$ Hz, $\text{H}^{4/5}$, $\text{C}_5\text{H}_4\text{N}$), 8.65 (d, $^3J(\text{H}^1, \text{H}^1) = 4.6$ Hz, $\text{H}^{3/6}$, $\text{C}_5\text{H}_4\text{N}$).

Synthesis of 1-($\text{C}_5\text{H}_4\text{NCH}$) C_9H_6 (4'). A solution of sodium methanolate (10.8 g, 200 mmol) in methanol (250 mL) was treated with indene (10 mL, 86 mmol) and 2-pyridinecarboxaldehyde (5.68 g, 53 mmol). The reaction mixture was heated under reflux for 1h and then stirred at room temperature overnight. The solution was diluted with water (300 mL) and extracted with pentane (5 × 200 mL). The combined organic layers were dried with magnesium sulfate and volatiles were vacuum evaporated on rotavapor. The crude product was purified by column chromatography on silica (hexane : Et_2O – 1 : 1). Yield: 5.22 g (25 mmol, 48%). Yellow crystals. Mp: 114 °C. Anal. Calcd. for $\text{C}_{15}\text{H}_{11}\text{N}$: C, 87.77; H, 5.40; N, 6.83. Found: C, 87.59; H, 5.36; N, 6.91. ^1H NMR (CDCl_3 ; 500.20 MHz): δ = 7.06 (dd, $^3J(\text{H}^1, \text{H}^1) = 5.6$ Hz, $^4J(\text{H}^1, \text{H}^1) = 1.5$ Hz, 1H, H^3 , C_9H_6), 7.21–7.34 (m, 1H of $\text{C}_5\text{H}_4\text{N}$, H^5 and 3H of C_9H_6 , H^{4-7}), 7.41 (s, 1H, $\text{C}_9\text{H}_6\text{CHC}_5\text{H}_4\text{N}$), 7.56 (d, $^3J(\text{H}^1, \text{H}^1) = 7.9$ Hz, 1H, H^3 , $\text{C}_5\text{H}_4\text{N}$), 7.65 (d, $^3J(\text{H}^1, \text{H}^1) = 5.6$ Hz, 1H, H^2 , C_9H_6), 7.71 (d, $^3J(\text{H}^1, \text{H}^1) = 7.3$ Hz, 1H, $\text{H}^{4/7}$, C_9H_6), 7.75 (ddd, $^3J(\text{H}^1, \text{H}^1) = 7.9$ Hz, $^3J(\text{H}^1, \text{H}^1) = 7.6$ Hz, $^4J(\text{H}^1, \text{H}^1) = 1.9$ Hz, 1H, H^4 , $\text{C}_5\text{H}_4\text{N}$), 8.75 (ddd, $^3J(\text{H}^1, \text{H}^1) = 4.8$ Hz, $^4J(\text{H}^1, \text{H}^1) = 1.7$ Hz, $^5J(\text{H}^1, \text{H}^1) = 0.8$ Hz, 1H, H^6 , $\text{C}_5\text{H}_4\text{N}$). $^{13}\text{C}\{^1\text{H}\}$ NMR (CDCl_3 ; 125.77 MHz): δ = 119.7 (1C, $\text{C}^{4/7}$, C_9H_6), 121.3 (1C, $\text{C}^{5/6}$, C_9H_6), 122.6 (1C, $\text{C}^{4/7}$, C_9H_6), 125.6 (1C, C^2 , $\text{C}_5\text{H}_4\text{N}$), 125.9 (1C, $\text{C}_9\text{H}_6\text{CHC}_5\text{H}_4\text{N}$), 126.2 (1C, C^3 , $\text{C}_5\text{H}_4\text{N}$), 127.6 (1C, C^2 , C_9H_6), 128.4 (1C, $\text{C}^{5/6}$, C_9H_6), 136.1 (1C, C^3 , C_9H_6), 136.9 (1C, C^4 , $\text{C}_5\text{H}_4\text{N}$), 150.0 (1C, C^6 , $\text{C}_5\text{H}_4\text{N}$), 137.8, 142.7, 143.2 (3 × 1C_q, C_9H_6), 155.7 (1C_q, C^2 , $\text{C}_5\text{H}_4\text{N}$). Single crystals suitable for X-ray diffraction analysis were prepared by a slow evaporation of Et_2O solution.

Synthesis of 1,3-($\text{C}_5\text{H}_4\text{NCH}_2$) C_9H_6 (5). A solution of 3-($\text{C}_5\text{H}_4\text{NCH}_2$) C_9H_7 (4; 5.18 g, 25 mmol) was cooled to 0 °C, treated with a solution of $^n\text{BuLi}$

in hexane (15.6 mL, 1.6 mol/L, 25 mmol) dropwise and stirred for 30 min. at this temperature. The reaction mixture was treated with $\text{C}_5\text{H}_4\text{NCH}_2\text{Cl}$ (3.10 g, 25 mmol) dropwise, stirred at room temperature overnight and then poured into distilled water (75 mL). Crude product was extracted with CH_2Cl_2 . Combined organic layers were dried with magnesium sulfate. The volatiles were evaporated on the rotavapor and crude product was purified by column chromatography on silica (ethyl acetate). Yield: 1.56 g (5.2 mmol, 21%). Pale yellow liquid. Anal. Calcd. for $\text{C}_{15}\text{H}_{11}\text{N}$: C, 86.50; H, 6.77; N, 6.73. Found: C, 86.67; H, 6.69; N, 6.85. ^1H NMR (CDCl_3 , 400.13 MHz): δ = 2.91 (dd, $^2J(\text{H}^1, \text{H}^1) = 13.5$ Hz, $^3J(\text{H}^1, \text{H}^1) = 8.8$ Hz, 1H, 1-($\text{C}_5\text{H}_4\text{NCH}_2$) C_9H_6), 3.25 (dd, $^2J(\text{H}^1, \text{H}^1) = 13.5$ Hz, $^3J(\text{H}^1, \text{H}^1) = 6.7$ Hz, 1H, 1-($\text{C}_5\text{H}_4\text{NCH}_2$) C_9H_6), 4.02 (dd, $^3J(\text{H}^1, \text{H}^1) = 8.8$ Hz, $^3J(\text{H}^1, \text{H}^1) = 6.7$ Hz, 1H, C_9H_6), 4.06 (s, 2H, 3-($\text{C}_5\text{H}_4\text{NCH}_2$) C_9H_6), 6.20 (s, 1H, H^2 , C_9H_6), 7.04–7.24 (m, 8H, $\text{H}^{3,4}$ of ($\text{C}_5\text{H}_4\text{NCH}_2$) C_9H_6 , H^{4-7} of C_9H_6), 7.51, 7.57 (2 × td, $^3J(\text{H}^1, \text{H}^1) = 7.6$ Hz, $^4J(\text{H}^1, \text{H}^1) = 1.5$ Hz, 2H, H^5 , $\text{C}_5\text{H}_4\text{N}$), 8.53, 8.59 (2 × d, $^3J(\text{H}^1, \text{H}^1) = 4.7$ Hz, 2H, H^6 , $\text{C}_5\text{H}_4\text{N}$). $^{13}\text{C}\{^1\text{H}\}$ NMR (CDCl_3 , 100.61 MHz): δ = 37.4, 40.4 (2 × 1C, CH_2), 49.2 (1C, C^1 , C_9H_6), 119.9, 121.4, 121.6, 122.9, 123.2, 123.7, 124.9, 126.7, 135.6, 136.4, 136.6, 149.3, 149.4 (13 × 1C, $\text{C}^{2,4-7}$ of C_9H_6 , C^{3-6} of ($\text{C}_5\text{H}_4\text{NCH}_2$) C_9H_6 , 140.9, 144.5, 147.9 (3 × 1C_q, $\text{C}^{3,3A,7A}$, C_9H_6), 159.5, 160.3 (2 × 1C_q, C^2 , ($\text{C}_5\text{H}_4\text{NCH}_2$) C_9H_6).

Synthesis of $[(\eta^3\text{-C}_3\text{H}_5)(\eta^5\text{-C}_5\text{H}_4\text{NCH}_2\text{C}_5\text{H}_4)\text{Mo}(\text{CO})_2]$ (7). A solution of 3 (1.57 g, 10 mmol) in THF (40 mL) was cooled to 0 °C, treated with a solution of $^n\text{BuLi}$ in hexane (6.55 μL , 1.6 mol/L, 10 mmol) dropwise and stirred for 30 min. at room temperature. The reaction mixture was cooled to –80 °C and treated with a solution of $[(\eta^3\text{-C}_3\text{H}_5)\text{Mo}(\text{CO})_2(\text{NCMe})_2\text{Cl}]$ (3.1 g, 10 mmol) in THF (30 mL) dropwise. The mixture was stirred at room temperature overnight. The volatiles were vacuum evaporated and crude product was extracted with hexane (3 × 70 mL) at 60 °C. The solvent was vacuum evaporated. The product was recrystallized from the mixture hexane/ Et_2O at –80 °C and vacuum dried. Yield: 1.88 g (5.4 mmol, 54%). Yellow viscous liquid. Anal. Calcd. for $\text{C}_{16}\text{H}_{15}\text{MoNO}_2$: C, 55.03; H, 4.33; N, 4.01. Found: C, 55.28; H, 4.48; N, 3.86. ^1H NMR (CDCl_3 , 400.13 MHz, 3.5 : 1 mixture of 7a (exo- C_3H_5) and 7b (endo- C_3H_5)): δ = 0.88 (d, $^3J(\text{H}^1, \text{H}^1) = 10.8$ Hz, 2H of a, H^{anti} , C_3H_5), 1.62 (d, $^3J(\text{H}^1, \text{H}^1) = 10.3$ Hz, 2H of b, H^{anti} , C_3H_5), 2.66 (d, $^3J(\text{H}^1, \text{H}^1) = 7.0$ Hz, 2H of a, H^{syn} , C_3H_5), 2.73 (s-br, 2H of b, H^{syn} , C_3H_5), 3.59 (m, 1H of b, H^{meso} , C_3H_5), 3.66 (s, 2H of a and 2H of b, CH_2), 3.88 (m, 1H of a, H^{meso} , C_3H_5), 5.12 (dd, $^3J(\text{H}^1, \text{H}^1) = 2.1$ Hz, $^4J(\text{H}^1, \text{H}^1) = 2.1$ Hz, 2H of a and 2H of b, C_5H_4), 5.21 (dd, $^3J(\text{H}^1, \text{H}^1) = 2.1$ Hz, $^4J(\text{H}^1, \text{H}^1) = 2.1$ Hz, 2H of a and 2H of b, C_5H_4), 7.09 (ddd, $^3J(\text{H}^1, \text{H}^1) = 7.5$ Hz, $^3J(\text{H}^1, \text{H}^1) = 4.9$ Hz, $^4J(\text{H}^1, \text{H}^1) = 0.8$ Hz, 1H of a and 1H of b, H^5 , $\text{C}_5\text{H}_4\text{N}$), 7.12 (d, $^3J(\text{H}^1, \text{H}^1) = 7.9$ Hz, 1H of a and 1H of b, H^3 , $\text{C}_5\text{H}_4\text{N}$), 7.56 (ddd, $^3J(\text{H}^1, \text{H}^1) = 7.9$ Hz, $^3J(\text{H}^1, \text{H}^1) = 7.5$ Hz, $^3J(\text{H}^1, \text{H}^1) = 1.8$ Hz, 1H of a and 1H of b, H^4 , $\text{C}_5\text{H}_4\text{N}$), 8.47 (ddd, $^3J(\text{H}^1, \text{H}^1) = 4.9$ Hz, $^4J(\text{H}^1, \text{H}^1) = 1.8$ Hz, $^5J(\text{H}^1, \text{H}^1) = 0.9$ Hz, 1H of a and 1H of b, H^6 , $\text{C}_5\text{H}_4\text{N}$). $^{13}\text{C}\{^1\text{H}\}$ NMR (CDCl_3 , 125.77 MHz): δ = 37.4 (1C of a and 1C of b, CH_2), 38.0 (2C of b, $\text{C}^{1,3}$, C_3H_5), 40.9 (2C of a, $\text{C}^{1,3}$, C_3H_5), 68.7 (1C of a, C^2 , C_3H_5), 89.8 (2C of a and 2C b, C_4H_5), 92.4 (2C of a and 2C b, C_4H_5), 111.0 (1C_q of a and 1C_q b, C_4H_5), 121.6 (1C of a and 1C b, C^5 , $\text{C}_5\text{H}_4\text{N}$), 122.7 (1C of a and 1C b, C^3 , $\text{C}_5\text{H}_4\text{N}$), 136.7 (1C of a and 1C b, C^4 , $\text{C}_5\text{H}_4\text{N}$), 149.2 (1C of a and 1C b, C^6 , $\text{C}_5\text{H}_4\text{N}$), 159.3 (1C_q of a and 1C_q b, C^2 , $\text{C}_5\text{H}_4\text{N}$), 237.6 (2C of a and 2C b, CO). IR(ATR; cm^{-1}): 1927 vs [$\nu_a(\text{CO})$], 1838 vs [$\nu_s(\text{CO})$]. Single crystals of 7 suitable for X-ray diffraction analysis were prepared by slow evaporation of hexane solution under inert atmosphere.

Synthesis of $[(\eta^3\text{-C}_3\text{H}_5)(\eta^5\text{-1-(C}_5\text{H}_4\text{NCH}_2\text{)}_2\text{C}_9\text{H}_6)\text{Mo}(\text{CO})_2]$ (8). Method A: The reaction was carried out as described for compound 7 but with indene derivative 4 (2.07 g; 10 mmol). Yield: 2.63 g (6.6 mmol, 66%). Method B: A solution of 4' (2.05 g, 10 mmol) in Et_2O (80 mL) was treated with a solution of Super-Hydride in THF (10 mL, 1.0 mol/L, 10 mmol). The reaction mixture was stirred overnight. The white precipitate was decanted, washed with Et_2O (3 × 10 mL) and vacuum dried. The white solid was dissolved in THF (40 mL), cooled to –80 °C and treated with a solution of $[(\eta^3\text{-C}_3\text{H}_5)\text{Mo}(\text{CO})_2(\text{NCMe})_2\text{Cl}]$ (3.1 g, 10 mmol) in THF (30 mL) dropwise. The reaction mixture was stirred at room temperature overnight. The volatiles were vacuum evaporated and crude product was extracted with hexane (3 × 70 mL) at 60 °C. The solvent was vacuum

evaporated. The product was recrystallized from mixture hexane/Et₂O at -80 °C and vacuum dried. Yield: 2.48 g (6.2 mmol, 62%). Yellow crystals. Mp: 64.7 °C. Anal. Calcd. for C₂₀H₁₇MoNO₂: C, 60.16; H, 4.29; N, 3.01. Found: C, 60.02; H, 4.39; N, 2.85. ¹H NMR (CDCl₃, 400.13 MHz, 3.8 : 1 mixture of **8a** (exo-C₃H₅) and **8b** (endo-C₃H₅): δ = -0.88 (d, ³J(¹H,¹H) = 10.9 Hz, 1H of **b**, H^{anti}, C₃H₅), -0.72 (d, ³J(¹H,¹H) = 10.7 Hz, 1H of **b**, H^{anti}, C₃H₅), 0.22 (m, 1H of **a**, H^{meso}, C₃H₅), 0.86 (d, ³J(¹H,¹H) = 11.1 Hz, 1H of **a**, H^{anti}, C₃H₅), 0.96 (d, ³J(¹H,¹H) = 11.2 Hz, 1H of **a**, H^{anti}, C₃H₅), 2.21 (d, ³J(¹H,¹H) = 7.3 Hz, 1H of **a**, H^{syn}, C₃H₅), 2.28 (d, ³J(¹H,¹H) = 7.4 Hz, 1H of **a**, H^{syn}, C₃H₅), 3.44–3.28 (m, 3H of **b**, H^{syn}, H^{meso}, C₃H₅), 4.35 (ABq, Δδ_{AB} = 0.06, ²J(¹H,¹H) = 15.5 Hz, 2H of **b**, CH₂), 4.39 (ABq, Δδ_{AB} = 0.24, ²J(¹H,¹H) = 15.5 Hz, 2H of **b**, CH₂), 5.73 (d, ³J(¹H,¹H) = 2.7 Hz, 1H of **b**, H², C₉H₆), 5.79 (d, ³J(¹H,¹H) = 2.7 Hz, 1H of **a**, H², C₉H₆), 5.83 (d, ³J(¹H,¹H) = 2.7 Hz, 1H of **b**, H³, C₉H₆), 5.89 (d, ³J(¹H,¹H) = 2.7 Hz, 1H of **a**, H³, C₉H₆), 6.88–7.28 (m, 6H of **a** and 6H of **b**, H⁴⁻⁷ of C₉H₆ and H^{3,5} of C₅H₄N), 7.57 (dd-br, ³J(¹H,¹H) = 7.8 Hz, ³J(¹H,¹H) = 7.6 Hz, 1H of **a** and 1H of **b**, H⁴, C₅H₄N), 8.50 (d-br, ³J(¹H,¹H) = 4.6 Hz, 1H of **a** and 1H of **b**, H⁶, C₅H₄N). IR (ATR; cm⁻¹): 1933 vs [ν_a(CO)], 1854 vs [ν_s(CO)]. When the reaction was carried out with **4-D**, **8-[D]** was obtained, for which the signals at 5.83 and 5.89 ppm in the ¹H NMR spectrum decreased in intensity (35 % of initial intensity) and those at 5.73 and 5.79 ppm were seen as a broadened singlet.

Synthesis of [(η³-C₃H₅)(η⁵-1,3-(C₅H₄NCH₂)₂C₉H₅)Mo(CO)₂] (9). The reaction was carried out as described for compound **7** but with indene derivative **5** (2.97 g; 10 mmol). Yield: 1.14 g (3.2 mmol, 32%). Yellow crystals. Mp: 133 °C. Anal. Calcd. for C₂₆H₂₂MoN₂O₂: C, 63.68; H, 4.52; N, 5.71. Found: C, 63.73; H, 4.59; N, 5.59. ¹H NMR (CDCl₃, 400.13 MHz, 3.5 : 1 mixture of **9a** (exo-C₃H₅) and **9b** (endo-C₃H₅): δ = -0.77 (d, ³J(¹H,¹H) = 10.6 Hz, 2H of **b**, H^{anti}, C₃H₅), 0.51 (tt, ³J(¹H,¹H) = 11.1 Hz, ³J(¹H,¹H) = 7.3 Hz, 1H of **a**, H^{meso}, C₃H₅), 0.88 (d, ³J(¹H,¹H) = 11.1 Hz, 2H of **a**, H^{anti}, C₃H₅), 2.16 (d, ³J(¹H,¹H) = 7.3 Hz, 2H of **a**, H^{syn}, C₃H₅), 3.23–3.43 (m, 3H of **b**, H^{syn}, H^{meso}, C₃H₅), 4.31 (ABq, Δδ_{AB} = 0.07, ²J(¹H,¹H) = 15.5 Hz, 2H of **a**, CH₂), 4.35 (ABq, Δδ_{AB} = 0.19, ²J(¹H,¹H) = 15.5 Hz, 2H of **b**, CH₂), 5.93 (s, 1H of **b**, H², C₉H₅), 5.97 (s, 1H of **a**, H², C₉H₅), 6.93 (dd, ³J(¹H,¹H) = 6.5 Hz, ⁴J(¹H,¹H) = 3.1 Hz, 2H of **b**, H⁴⁻⁷, C₉H₅), 7.00 (dd, ³J(¹H,¹H) = 6.5 Hz, ⁴J(¹H,¹H) = 3.1 Hz, 2H of **a**, H⁴⁻⁷, C₉H₅), 7.09–7.22 (m, 6H of **a** and 6H of **b**, H⁴⁻⁷ of C₉H₅ and H^{3,5} of C₅H₄N), 7.56 (m, 2H of **a** and 2H of **b**, H⁴, C₅H₄N), 8.50 (m, 2H of **a** and 2H of **b**, H⁶, C₅H₄N). IR (ATR; cm⁻¹): 1934 vs [ν_a(CO)], 1853 vs [ν_s(CO)]. Raman (cm⁻¹): 1919(3) [ν_a(CO)], 1838(10) [ν_s(CO)]. Single crystals of **9** suitable for X-ray diffraction analysis were prepared by sublimation in vacuum-sealed (1 Pa) ampule at 110 °C.

[(η⁵-C₅H₄NHCH₂C₅H₄)Mo(CO)₂(NCMe)₂][BF₄]₂ (10). A solution of **7** (0.7 g, 2 mmol) in MeCN (5 mL) was cooled to 0 °C and treated with HBF₄·Et₂O (550 μL, 4 mmol) dropwise. The reaction mixture was stirred at room temperature overnight. The volatiles were vacuum evaporated. Crude product was washed with Et₂O (2 × 5 mL), recrystallized from the mixture MeCN/Et₂O and vacuum dried. Yield 0.49 g (0.86 mmol, 43%). Red crystals. Mp: 137 °C (dec). Anal. Calcd. for C₁₇H₁₇B₂F₈MoN₃O₂: C, 36.15; H, 3.03; N, 7.44. Found: C, 36.25; H, 3.16; N, 7.29. ¹H NMR (CD₃CN, 400.13 MHz): δ = 2.49 (s, 6H, NCCCH₃), 4.06 (s, 2H, CH₂), 5.66 (dd, ³J(¹H,¹H) = 2.2 Hz, ⁴J(¹H,¹H) = 2.1 Hz, 2H, C₅H₄), 6.96 (dd, ³J(¹H,¹H) = 2.2 Hz, ⁴J(¹H,¹H) = 2.1 Hz, 2H, C₅H₄), 7.94–7.99 (m, 2H, H^{3,5}, C₅H₄NH), 8.56 (ddd, ³J(¹H,¹H) = 8.0 Hz, ³J(¹H,¹H) = 8.0 Hz, ⁴J(¹H,¹H) = 1.0 Hz, 1H, H⁴, C₅H₄NH), 8.65 (t-br, ³J(¹H,¹H) = 4.8 Hz, 1H, H⁶, C₅H₄NH), 13.2 (s-br, 1H, C₅H₄NH). IR (ATR; cm⁻¹): 2324 vs [ν_a(CN)], 2296 vs [ν_s(CN)], 1981 vs [ν_a(CO)], 1905 vs [ν_s(CO)], 1026 vs-br [ν(BF)]. Raman (cm⁻¹): 2323(5) [ν_a(CN)], 2289(10) [ν_s(CN)], 1984(4) [ν_a(CO)], 1917(8) [ν_s(CO)]. Single crystals of **10** suitable for X-ray diffraction analysis were prepared by diffusion of hexane into saturated solution of **10** in CH₂Cl₂.

[(η⁵-κN-C₅H₄NCH₂C₅H₄)Mo(CO)₂(NCMe)][BF₄] (11). A solution of **7** (0.7 g, 2 mmol) in the mixture of CH₂Cl₂ (5 mL) and MeCN (105 μL, 2 mmol) was cooled to 0 °C and treated with HBF₄·Et₂O (225 μL, 2 mmol) dropwise. The reaction mixture was stirred at room temperature overnight. The volatiles were vacuum evaporated. The remaining solid was dissolved in acetone (10 mL) and stirred overnight. The volatiles

were vacuum evaporated, crude product was recrystallized from the mixture acetone/Et₂O and vacuum dried. Yield 0.64 g (1.48 mmol, 74%). Purple crystals. Mp: 140 °C (dec). Anal. Calcd. for C₁₅H₁₃BF₄MoN₂O₂: C, 41.31; H, 3.00; N, 6.42. Found: C, 41.16; H, 3.09; N, 6.50. Positive-ion MS (MeCN): *m/z* = 351 (100%) [M]⁺, 310 [M - MeCN]⁺. ¹H NMR (acetone-d₆, 400.13 MHz): δ = 2.66 (s, 3H, NCCCH₃), 4.39 (ABq, Δδ_{AB} = 0.09 ppm, ²J(¹H,¹H) = 18.2 Hz, 2H, CH₂), 5.19 (ddd, ³J(¹H,¹H) = 2.6 Hz, ³J(¹H,¹H) = 2.6 Hz, ⁴J(¹H,¹H) = 1.6 Hz, 1H, C₅H₄), 5.80 (ddd, ³J(¹H,¹H) = 2.7 Hz, ³J(¹H,¹H) = 2.7 Hz, ⁴J(¹H,¹H) = 1.6 Hz, 1H, C₅H₄), 6.23 (ddd, ³J(¹H,¹H) = 2.7 Hz, ⁴J(¹H,¹H) = 1.6 Hz, ⁴J(¹H,¹H) = 1.6 Hz, 1H, C₅H₄), 6.65 (ddd, ³J(¹H,¹H) = 2.8 Hz, ⁴J(¹H,¹H) = 1.6 Hz, ⁴J(¹H,¹H) = 1.6 Hz, 1H, C₅H₄), 7.38 (dd, ³J(¹H,¹H) = 7.5 Hz, ³J(¹H,¹H) = 5.8 Hz, 1H, H⁵, C₅H₄N), 7.48 (ddd, ³J(¹H,¹H) = 8.1 Hz, ⁴J(¹H,¹H) = 1.5 Hz, ⁵J(¹H,¹H) = 0.8 Hz, 1H, H³, C₅H₄N), 7.95 (ddd, ³J(¹H,¹H) = 7.9 Hz, ³J(¹H,¹H) = 7.9 Hz, ⁴J(¹H,¹H) = 1.6 Hz, 1H, H⁴, C₅H₄N), 8.43 (ddd, ³J(¹H,¹H) = 5.9 Hz, ⁴J(¹H,¹H) = 1.5 Hz, ⁵J(¹H,¹H) = 0.7 Hz, 1H, H⁶, C₅H₄N). ¹³C{¹H} NMR (acetone-d₆, 125.77 MHz): δ = 36.3 (1C, CH₂), 86.7, 87.8, 88.1, 104.0 (4 × 1C, C₅H₄), 124.7 (1C, C⁵, C₅H₄N), 125.8 (1C, C³, C₅H₄N), 133.1 (1C_q, C₅H₄), 140.2 (1C, C⁴, C₅H₄N), 155.6 (1C, C⁶, C₅H₄N), 175.8 (1C_q, C², C₅H₄N), 248.8, 251.8 (2 × 1C, CO). IR (ATR; cm⁻¹): 2285 vs [ν(CN)], 1982 vs [ν_a(CO)], 1866 vs [ν_s(CO)], 1030 vs-br [ν(BF)]. Raman (cm⁻¹): 2285(6) [ν(CN)], 1982(7) [ν_a(CO)], 1898(10) [ν_s(CO)]. Single crystals of **11** suitable for X-ray diffraction analysis were prepared by diffusion of hexane into saturated solution of **11** in CH₂Cl₂.

Synthesis of [(η⁵-κN-C₅H₄NCH₂C₅H₄)Mo(CO)₂(py)][BF₄] (12). A solution of **11** (0.87 g, 2 mmol) in CH₂Cl₂ (5 mL) was treated with pyridine (1 mL, 12 mmol) and stirred at room temperature overnight. The volatiles were vacuum evaporated. Crude product was washed with Et₂O (2 × 10 mL), recrystallized from the mixture CH₂Cl₂/Et₂O and vacuum dried. Yield: 0.85 g (1.8 mmol, 90%). Mp: 130 °C (dec). Red crystals. Anal. Calcd. for C₁₈H₁₅BF₄MoN₂O₂: C, 45.60; H, 3.19; N, 5.91. Found: C, 45.73; H, 3.22; N, 5.83. Positive-ion MS (MeCN): *m/z* = 389 (100%) [M]⁺, 351 [M - py + MeCN]⁺, 310 [M - py]⁺. ¹H NMR (acetone-d₆, 400.13 MHz): δ = 4.40, 4.70 (2 × d, ²J(¹H,¹H) = 18.2 Hz), 2H, CH₂), 5.35 (ddd, ³J(¹H,¹H) = 2.8 Hz, ³J(¹H,¹H) = 2.8 Hz, ⁴J(¹H,¹H) = 1.6 Hz, 1H, C₅H₄), 5.89 (ddd, ³J(¹H,¹H) = 2.7 Hz, ³J(¹H,¹H) = 2.7 Hz, ⁴J(¹H,¹H) = 1.6 Hz, 1H, C₅H₄), 6.16 (ddd, ³J(¹H,¹H) = 2.9 Hz, ⁴J(¹H,¹H) = 1.6 Hz, ⁴J(¹H,¹H) = 1.6 Hz, 1H, C₅H₄), 6.77 (ddd, ³J(¹H,¹H) = 2.9 Hz, ⁴J(¹H,¹H) = 1.6 Hz, ⁴J(¹H,¹H) = 1.6 Hz, 1H, C₅H₄), 7.17 (dd, ³J(¹H,¹H) = 7.5 Hz, ³J(¹H,¹H) = 6.0 Hz, 1H, H⁵, C₅H₄N), 7.53 (ddd, ³J(¹H,¹H) = 8.1 Hz, ⁴J(¹H,¹H) = 1.5 Hz, ⁵J(¹H,¹H) = 0.7 Hz, 1H, H³, C₅H₄N), 7.61 (dt, ³J(¹H,¹H) = 7.7 Hz, ³J(¹H,¹H) = 6.4 Hz, 2H, H^{3,5}, C₅H₄N), 7.87 (dd, ³J(¹H,¹H) = 7.8 Hz, ³J(¹H,¹H) = 7.8 Hz, ⁴J(¹H,¹H) = 1.6 Hz, 1H, H⁴, C₅H₄N), 8.07 (tt, ³J(¹H,¹H) = 7.7 Hz, ⁴J(¹H,¹H) = 1.5 Hz, 1H, H⁴, C₅H₄N), 8.19 (d, ³J(¹H,¹H) = 5.9 Hz, ⁴J(¹H,¹H) = 1.5 Hz, ⁵J(¹H,¹H) = 0.7 Hz, 1H, H⁶, C₅H₄N), 9.11 (dd, ³J(¹H,¹H) = 6.4 Hz, ⁴J(¹H,¹H) = 1.5 Hz, 2H, H^{2,6}, C₅H₄N). ¹³C{¹H} NMR (acetone-d₆, 125.77 MHz): δ = 36.6 (1C, CH₂), 86.5, 87.1, 88.1, 106.8 (4 × 1C, C₅H₄), 124.7 (1C, C⁵, C₅H₄N), 126.1 (1C, C³, C₅H₄N), 127.7 (2C, C^{3,5}, C₅H₄N), 133.3 (1C_q, C₅H₄), 140.3 (1C, C⁴, C₅H₄N), 140.5 (1C, C⁴, C₅H₄N), 154.5 (1C, C⁶, C₅H₄N), 158.3 (2C, C^{2,6}, C₅H₄N), 175.4 (1C_q, C², C₅H₄N), 249.5, 250.1 (2 × 1C, CO). IR (ATR; cm⁻¹): 1997 vs [ν_a(CO)], 1840 vs [ν_s(CO)], 1030 vs-br [ν(BF)]. Raman (cm⁻¹): 2009(4) [ν_a(CO)], 2003(4) [ν_a(CO)], 1851(10) [ν_s(CO)]. Single crystals of **12** suitable for X-ray diffraction analysis were prepared by diffusion of hexane into saturated solution of **12** in CH₂Cl₂.

Synthesis of [(η⁵-κN-C₅H₄NCH₂C₅H₄)Mo(CO)₂Cl][BF₄] (13). A solution of **11** (0.87 g, 2 mmol) in acetone (5 mL) was treated with [Me₄N]Cl (0.22 g, 2 mmol) and stirred at room temperature overnight. The volatiles were vacuum evaporated and remaining solid was extracted with CH₂Cl₂ (7 mL). The white precipitate of [Me₄N][BF₄] was filtrated off and the volatiles of the filtrate were vacuum evaporated. The crude product was recrystallized from acetone/Et₂O and vacuum dried. Yield: 0.63 g (1.83 mmol, 92%). Purple crystals. Mp: 150 °C (dec). Anal. Calcd. for C₁₃H₁₀ClMoNO₂: C, 45.44; H, 2.93; N, 4.07. Found: C, 45.62; H, 2.85; N, 3.94. ¹H NMR (acetone-d₆, 400.13 MHz): δ = 4.46 (ABq, Δδ_{AB} = 0.05 ppm, ²J(¹H,¹H) = 18.0 Hz, 2H, CH₂), 5.98 (ddd, ³J(¹H,¹H) = 2.5 Hz, ³J(¹H,¹H) = 2.5 Hz, ⁴J(¹H,¹H) = 1.6 Hz, 1H, C₅H₄), 5.62 (ddd, ³J(¹H,¹H) = 2.7 Hz, ³J(¹H,¹H) = 2.7 Hz, ⁴J(¹H,¹H) = 1.6 Hz, 1H, C₅H₄), 6.01 (ddd,

$^3J(^1H, ^1H) = 2.9$ Hz, $^4J(^1H, ^1H) = 1.7$ Hz, $^4J(^1H, ^1H) = 1.7$ Hz, 1H, C₅H₄), 6.03 (ddd, $^3J(^1H, ^1H) = 2.8$ Hz, $^4J(^1H, ^1H) = 1.7$ Hz, $^4J(^1H, ^1H) = 1.7$ Hz, 1H, C₅H₄), 7.22 (dd, $^3J(^1H, ^1H) = 7.6$ Hz, $^3J(^1H, ^1H) = 5.7$ Hz, 1H, H⁵, C₅H₄N), 7.31 (d, $^3J(^1H, ^1H) = 7.9$ Hz, 1H, H³, C₅H₄N), 7.79 (td, $^3J(^1H, ^1H) = 7.8$ Hz, $^4J(^1H, ^1H) = 1.7$ Hz, 1H, H⁴, C₅H₄N), 8.34 (d, $^3J(^1H, ^1H) = 5.7$ Hz, 1H, H⁶, C₅H₄N). $^{13}C\{^1H\}$ NMR (CD₃CN, 125.77 MHz): $\delta = 36.2$ (1C, CH₂), 86.2, 87.02, 87.04, 108.3 (4 × 1C, C₅H₄), 123.7 (1C, C⁵, C₅H₄N), 124.6 (1C, C³, C₅H₄N), 131.1 (1C_q, C₅H₄), 139.2 (1C, C⁴, C₅H₄N), 156.7 (1C, C⁶, C₅H₄N), 173.6 (1C_q, C², C₅H₄N), 252.8, 264.3 (2 × 1C, CO). IR (ATR; cm⁻¹): 1945 vs [ν_a (CO)], 1827 vs [ν_s (CO)]. Raman (cm⁻¹): 1950(8) [ν_a (CO)], 1846(10) [ν_s (CO)]. Single crystals of **13** suitable for X-ray diffraction analysis were prepared by diffusion of hexane into saturated solution of **13** in CH₂Cl₂.

Synthesis of $[\{\eta^3\text{-}\kappa\text{N-1-(C}_5\text{H}_4\text{NCH}_2\text{)}\text{C}_9\text{H}_6\}\text{Mo(CO)}_2(\text{NCMe}_2)_2\text{][BF}_4\text{]}^-$ (**14**).

A solution of **8** (0.8 g, 2 mmol) in the mixture of CH₂Cl₂ (5 mL) and MeCN (208 μ L, 4 mmol) was cooled to 0 °C and treated with HBF₄·Et₂O (275 μ L, 2 mmol) dropwise. The reaction mixture was stirred at room temperature overnight and volatiles were vacuum evaporated. The remaining solid was dissolved in acetone (7 mL), stirred at room temperature overnight and vacuum evaporated. This step was repeated with MeCN. The obtained crude product was washed with CH₂Cl₂ (5 mL) and recrystallized from MeCN/Et₂O and vacuum dried. Yield: 0.59 (1.12 mmol, 56%). Mp: 138 °C (dec). Red crystals. Anal. Calcd. for C₂₁H₁₈BF₄MoN₃O₂: C, 47.85; H, 3.44; N, 7.97. Found: C, 47.61; H, 3.42; N, 7.87. Positive-ion MS (MeCN): $m/z = 414$ [M – CO]⁺, 401 (100%) [M – MeCN]⁺, 373 [M – MeCN – CO]⁺, 360 [M – 2MeCN]⁺. ^1H NMR (CD₃CN, 400.13 MHz): $\delta = 4.03$, 4.27 (2 × d, $^2J(^1H, ^1H) = 19.8$ Hz, 2H, CH₂), 5.14 (d, $^3J(^1H, ^1H) = 3.9$ Hz, 1H, H³, C₉H₆), 6.45–6.61 (m, 4H, H^{4–7}, C₉H₆), 6.83 (d, $^3J(^1H, ^1H) = 3.9$ Hz, 1H, H², C₉H₆), 7.33 (dd, $^3J(^1H, ^1H) = 7.6$ Hz, $^3J(^1H, ^1H) = 5.6$ Hz, 1H, H⁵, C₅H₄N), 7.62 (d, $^3J(^1H, ^1H) = 7.8$ Hz, 1H, H³, C₅H₄N), 7.84 (d, $^3J(^1H, ^1H) = 5.6$ Hz, 1H, H⁶, C₅H₄N), 7.93 (ddd, $^3J(^1H, ^1H) = 7.7$ Hz, $^3J(^1H, ^1H) = 7.7$ Hz, $^4J(^1H, ^1H) = 1.6$ Hz, 1H, H⁴, C₅H₄N). $^{13}C\{^1H\}$ NMR (CD₃CN, 125.77 MHz): $\delta = 35.8$ (1C, CH₂), 73.1 (1C, C³, C₉H₆), 86.0 (1C_q, C¹, C₉H₆), 98.8 (1C, C², C₉H₆), 116.1, 117.2, 124.8, 124.9 (4 × 1C, C^{4–7}, C₉H₆), 123.8 (1C, C⁵, C₅H₄N), 124.5 (1C, C⁶, C₅H₄N), 139.5 (1C, C⁴, C₅H₄N), 146.0, 147.6 (2 × 1C_q, C^{3a,7a}, C₉H₆), 150.2 (1C, C⁶, C₅H₄N), 161.8 (1C_q, C², C₅H₄N), 221.1, 221.4 (2 × 1C, CO). IR (ATR; cm⁻¹): 2317 vs [ν_a (CN)], 2284 vs [ν_s (CN)], 1967 vs [ν_a (CO)], 1904 vs [ν_s (CO)], 1029 vs-br [ν (BF)], Raman (cm⁻¹): 2316(3) [ν_a (CN)], 2284(10) [ν_s (CN)], 1988(2) [ν_a (CO)], 1900(4) [ν_s (CO)]. Single crystals of **14**·CH₂Cl₂ suitable for X-ray diffraction analysis were prepared by diffusion of Et₂O into saturated solution of **14** in CH₂Cl₂. When the reaction was carried out with **8**·[**D**], **14**·[**D**] was obtained, for which the signal at 5.14 ppm in the ^1H NMR spectrum decreased in intensity (35 % of initial intensity) and that at 6.83 ppm was seen as a broadened singlet.

Synthesis of $[\{\eta^3\text{-}\kappa\text{N-1-(C}_5\text{H}_4\text{NCH}_2\text{)}\text{C}_9\text{H}_6\}\text{Mo(CO)}_2(\text{phen})\text{][BF}_4\text{]}^-$ (**15**).

A solution of **14** (1.05, 2 mmol) in MeCN (5 mL) was treated with 1,10-phenanthroline (0.36 g, 2 mmol). The reaction mixture was stirred at room temperature overnight. The volatiles were vacuum evaporated. Crude product was washed with CH₂Cl₂ (3 × 5 mL), recrystallized from MeCN/Et₂O and vacuum dried. Yield: 1.11 g (1.78 mmol, 89%). Brown crystals. Mp: 155 °C (dec). Anal. Calcd. for C₂₉H₂₀BF₄MoN₃O₂: C, 55.71; H, 3.22; N, 6.72. Found: C, 55.55; H, 3.09; N, 6.64. Positive-ion MS (MeCN): $m/z = 540$ (100%) [M]⁺, 512 [M – CO]⁺, 484 [M – 2CO]⁺. ^1H NMR (acetone-d₆, 400.13 MHz): $\delta = 4.37$, 4.66 (2 × d, $^2J(^1H, ^1H) = 19.8$ Hz, 2H, CH₂), 5.51 (d, $^3J(^1H, ^1H) = 3.9$ Hz, 1H, H³, C₉H₆), 5.99 (ddd, $^3J(^1H, ^1H) = 5.2$ Hz, $^4J(^1H, ^1H) = 1.1$ Hz, $^4J(^1H, ^1H) = 1.1$ Hz, 1H, H⁶, C₅H₄N), 6.51–6.70 (m, 2H of C₉H₆ (H^{4–7}) and 2H of C₅H₄N (H^{4,5})), 6.71 (dd, $^3J(^1H, ^1H) = 7.2$ Hz, $^4J(^1H, ^1H) = 0.7$ Hz, H³, C₅H₄N), 7.40 (d, $^3J(^1H, ^1H) = 3.9$ Hz, 1H, H², C₉H₆), 7.81 (m, 2H, H^{4–7}, C₉H₆), 8.14 (dd, $^3J(^1H, ^1H) = 8.2$ Hz, $^3J(^1H, ^1H) = 5.2$ Hz, 1H, H^{3/8}, C₁₂H₈N₂), 8.39 (dd, $^3J(^1H, ^1H) = 8.3$ Hz, $^3J(^1H, ^1H) = 5.2$ Hz, 1H, H^{3/8}, C₁₂H₈N₂), 8.43 (ABq, $\Delta\delta_{AB} = 0.04$ ppm, $^3J(^1H, ^1H) = 8.7$ Hz, 2H, H^{5/6}, C₁₂H₈N₂), 8.93 (dd, $^3J(^1H, ^1H) = 8.2$ Hz, $^4J(^1H, ^1H) = 1.3$ Hz, 1H, H^{4/7}, C₁₂H₈N₂), 9.11 (dd, $^3J(^1H, ^1H) = 8.3$ Hz, $^4J(^1H, ^1H) = 1.4$ Hz, 1H, H^{4/7}, C₁₂H₈N₂), 9.51 (dd, $^3J(^1H, ^1H) = 5.2$ Hz, $^4J(^1H, ^1H) = 1.3$ Hz, 1H, H^{2/9}, C₁₂H₈N₂), 10.1 (dd, $^3J(^1H, ^1H) = 5.2$ Hz, $^4J(^1H, ^1H) = 1.3$ Hz, 1H, H^{2/9}, C₁₂H₈N₂). $^{13}C\{^1H\}$ NMR (CD₃CN, 125.77 MHz): $\delta = 36.8$ (1C, CH₂), 73.0 (1C, C³, C₉H₆), 86.5 (1C_q, C¹, C₉H₆), 98.6

(1C, C², C₉H₆), 116.6 (1C, C³, C₄H₅N), 118.4, 124.8, 125.7, 125.9, 126.0 (5 × 1C, C₄H₅N (C^{4,5}), C₉H₆ (C^{4–7}), 126.5 (1C, C^{3/8}, C₁₂H₈N₂), 127.5 (1C, C^{3/8}, C₁₂H₈N₂), 128.9 (1C, C^{5/6}, C₁₂H₈N₂), 129.4 (1C, C^{5/6}, C₁₂H₈N₂), 132.0, 132.2, 142.0, 144.7 (4 × 1C_q, C₁₂H₈N₂), 140.2 (1C, C^{4/7}, C₁₂H₈N₂), 140.4 (1C, C^{4–7}, C₉H₆), 141.4 (1C, C^{4/7}, C₁₂H₈N₂), 147.4, 148.6 (2 × 1C_q, C^{3a,7a}, C₉H₆), 147.9 (1C, C⁶, C₄H₅N), 153.8 (1C, C^{2/9}, C₁₂H₈N₂), 158.5 (1C, C^{2/9}, C₁₂H₈N₂), 163.5 (1C_q, C², C₄H₅N), 224.7, 222.4 (2 × 1C, CO). IR (ATR; cm⁻¹): 1921 vs [ν_a (CO)], 1861 vs [ν_s (CO)], 1030 vs-br [ν (BF)]. Raman (cm⁻¹): 1941(10) [ν_a (CO)], 1846(5) [ν_s (CO)]. Single crystals of **15** suitable for X-ray diffraction analysis were prepared by diffusion of Et₂O into saturated solution of **15** in MeCN. When the reaction was carried out with **14**·[**D**], **15**·[**D**] was obtained, for which the signal at 5.51 ppm in the ^1H NMR spectrum decreased in intensity (35 % of initial intensity) and that at 7.40 ppm was seen as a broadened singlet.

Synthesis of $[\text{Me}_4\text{N}][\{\eta^3\text{-}\kappa\text{N-1-(C}_5\text{H}_4\text{NCH}_2\text{)}\text{C}_9\text{H}_6\}\text{Mo(CO)}_2\text{Cl}_2]$ (**16**).

A solution of **14** (1.05, 2 mmol) in acetone (5 mL) was treated with [Me₄N]Cl (440 mg, 4 mmol). The reaction mixture was stirred at room temperature overnight. The volatiles were vacuum evaporated. The remaining solid was extracted with CH₂Cl₂ (7 mL) and white precipitate of [Me₄N][BF₄] was filtrated off. The volatiles of the filtrate were vacuum evaporated. Crude product was recrystallized from CH₂Cl₂/Et₂O and vacuum dried. Yield: 0.78 g (1.56 mmol, 78%). Mp: 147 °C (dec). Light orange crystals. Anal. Calcd. for C₂₁H₂₄Cl₂MoN₃O₂: C, 50.12; H, 4.81; N, 5.57. Found: C, 50.04; H, 4.88; N, 5.43. Negative-ion MS (MeCN): $m/z = 429$ (100%) [M]⁻. ^1H NMR (acetone-d₆, 500.20 MHz): $\delta = 3.43$ (s, 12H, (CH₃)₄N), 3.74, 4.04 (2 × d, $^2J(^1H, ^1H) = 19.1$ Hz, 2H, CH₂), 4.58 (d, $^3J(^1H, ^1H) = 3.9$ Hz, 1H, H³, C₉H₆), 6.24–6.37 (m, 4H, H^{4–7}, C₉H₆), 6.88 (d, $^3J(^1H, ^1H) = 3.9$ Hz, 1H, H², C₉H₆), 7.14 (dd, $^3J(^1H, ^1H) = 7.6$ Hz, $^3J(^1H, ^1H) = 5.6$ Hz, 1H, H⁵, C₅H₄N), 7.47 (d, $^3J(^1H, ^1H) = 7.8$ Hz, 1H, H³, C₅H₄N), 7.77 (ddd, $^3J(^1H, ^1H) = 7.8$ Hz, $^3J(^1H, ^1H) = 7.6$ Hz, $^4J(^1H, ^1H) = 1.7$ Hz, 1H, H⁴, C₅H₄N), 8.58 (dd, $^3J(^1H, ^1H) = 5.6$ Hz, $^4J(^1H, ^1H) = 1.5$ Hz, 1H, H⁶, C₅H₄N). IR (ATR; cm⁻¹): 1928 vs [ν_a (CO)], 1842 vs [ν_s (CO)]. Single crystals of **16**· $\frac{1}{2}$ Me₂CO suitable for X-ray diffraction analysis were prepared by diffusion of Et₂O into saturated solution of **16** in acetone. When the reaction was carried out with **14**·[**D**], **16**·[**D**] was obtained, for which the signal at 4.58 ppm in the ^1H NMR spectrum decreased in intensity (35 % of initial intensity) and that at 6.88 ppm was seen as a broadened singlet.

Synthesis of $[\{\eta^3\text{-}\kappa\text{N-1-(C}_5\text{H}_4\text{NCH}_2\text{)}\text{-3-(C}_5\text{H}_4\text{NHCH}_2\text{)}\text{C}_9\text{H}_5\}\text{Mo(CO)}_2(\text{NCMe}_2)_2\text{][BF}_4\text{]}^-$ (**17**).

A solution of **9** (0.98 g, 2 mmol) in MeCN (5 mL) was cooled to 0 °C and treated with HBF₄·Et₂O (0.82 mL, 6 mmol) dropwise. The reaction mixture was stirred at room temperature overnight. The volatiles were vacuum evaporated and remaining solid was washed with Et₂O (5 mL) and CH₂Cl₂ (5 mL). Crude product was recrystallized from MeCN/Et₂O and vacuum dried. Yield: 1.08 g (1.54 mmol, 77%). Red crystals. Mp: 133 °C (dec). Anal. Calcd. for C₂₇H₂₃B₂F₄MoN₄O₂: C, 46.00; H, 3.29; N, 4.75. Found: C, 45.88; H, 3.32; N, 4.84. ^1H NMR (CD₃CN, 400.13 MHz): $\delta = 4.05$, 4.33 (2 × d, $^2J(^1H, ^1H) = 19.9$ Hz, 2H, C₅H₄NCH₂), 4.18 (ABq, $\Delta\delta_{AB} = 0.04$ ppm, $^2J(^1H, ^1H) = 16.9$ Hz, 2H, C₅H₄NCH₂), 6.33 (d, $^3J(^1H, ^1H) = 7.2$ Hz, 1H, H^{4/7}, C₉H₅), 6.45 (dd, $^3J(^1H, ^1H) = 7.5$ Hz, $^3J(^1H, ^1H) = 7.3$ Hz, 1H, H^{5/6}, C₉H₅), 6.58 (dd, $^3J(^1H, ^1H) = 7.5$ Hz, $^3J(^1H, ^1H) = 7.2$ Hz, 1H, H^{5/6}, C₉H₅), 6.64 (d, $^3J(^1H, ^1H) = 7.1$ Hz, 1H, H^{4/7}, C₉H₅), 7.18 (s, 1H, H², C₉H₅), 7.29–7.55 (m, 4H of C₅H₄N and 4H of C₅H₄NH), 13.1 (m, 1H, C₅H₄NH). IR (ATR; cm⁻¹): 1958 vs [ν_a (CO)], 1873 vs [ν_s (CO)].

Synthesis of $[\{\eta^3\text{-}\kappa\text{N,N-1-3-(C}_5\text{H}_4\text{NCH}_2\text{)}_2\text{C}_9\text{H}_5\}\text{Mo(CO)}_2(\text{NCMe}_2)\text{][BF}_4\text{]}^-$ (**18**).

Complex **17** (0.49, 1 mmol) was dissolved in pyridine (5 mL). The reaction mixture was stirred at room temperature overnight. The excess of the pyridine was vacuum evaporated and remaining solid was extracted with CH₂Cl₂ (7 mL). The white precipitate of the pyridinium salt was filtrated off and volatiles of the filtrate were vacuum evaporated. Crude product was recrystallized from MeCN/Et₂O and vacuum dried. Yield: 0.27 g (0.46 mmol, 46%). Red crystals. Mp: 137 °C (dec). Anal. Calcd. for C₂₅H₂₀BF₄MoN₃O₂: C, 52.02; H, 3.49; N, 7.28. Found: C, 52.10; H, 3.41; N, 7.44. Positive-ion MS (MeCN): 492 (100%) [M]⁺, 464 [M – CO]⁺, 451 [M – MeCN]⁺, 423 [M – CO – MeCN]⁺, 395 [M – 2CO – MeCN]⁺. ^1H NMR (CD₃CN, 500.20 MHz): $\delta = 4.04$, 4.31 (2 × d, $^3J(^1H, ^1H)$

FULL PAPER

WILEY-VCH

= 19.6 Hz, 4H, CH₂), 6.38 (s, 1H, H², C₉H₅), 6.58 (m, 4H, H⁴⁻⁷, C₉H₅), 7.34 (dd, ³J(¹H,¹H) = 7.6 Hz, ³J(¹H,¹H) = 5.8 Hz, 2H, H⁵, C₅H₄N), 7.60 (d, ³J(¹H,¹H) = 8.0 Hz, 2H, H³, C₅H₄N), 7.90 (dd, ³J(¹H,¹H) = 8.0 Hz, ³J(¹H,¹H) = 7.6 Hz, 2H, H⁴, C₅H₄N), 8.05 (d, ³J(¹H,¹H) = 5.8 Hz, 2H, H⁶, C₅H₄N). IR (ATR; cm⁻¹): 1952 vs [ν_a(CO)], 1874 vs [ν_s(CO)]. Single crystals of **18** suitable for X-ray diffraction analysis were prepared by diffusion of Et₂O into saturated solution of **14** in MeCN.

Synthesis of [(η³-κN,N-1,3-(C₅H₄NCH₂)₂C₉H₅)Mo(CO)₂Cl] (19**).** A solution of **17** (0.58 g, 1 mmol) in acetone (5 mL) was treated with [Me₄N]Cl (0.11 g, 1 mmol). The reaction mixture was stirred at room temperature overnight. The light brown solution was decanted. Remaining orange precipitate was washed with methanol (3 × 5 mL) and vacuum dried. Yield: 0.38 g (0.78 mmol, 78 %). Orange crystals. Mp: 139 °C (dec). Anal. Calcd. for C₂₃H₁₇ClMoN₂O₂: C, 56.98; H, 3.54; N, 5.78. Found: C, 57.18; H, 3.45; N, 5.65. ¹H NMR (DMSO-d₆, 500.20 MHz): δ = 3.82, 4.21 (2 × d, ³J(¹H,¹H) = 19.4 Hz, 4H, CH₂), 6.26 (s, 1H, H², C₉H₅), 6.46 (m, 4H, H⁴⁻⁷, C₉H₅), 7.37 (dd, ³J(¹H,¹H) = 7.4 Hz, ³J(¹H,¹H) = 5.6 Hz, 2H, H⁵, C₅H₄N), 7.62 (d, ³J(¹H,¹H) = 7.7 Hz, 2H, H³, C₅H₄N), 7.91 (ddd, ³J(¹H,¹H) = 7.7 Hz, ³J(¹H,¹H) = 7.4 Hz, ⁴J(¹H,¹H) = 1.6 Hz, 2H, H⁴, C₅H₄N), 8.38 (dd, ³J(¹H,¹H) = 5.6 Hz; ⁴J(¹H,¹H) = 1.3 Hz; 2H, H⁶, C₅H₄N). IR (ATR; cm⁻¹): 1935 vs [ν_a(CO)], 1862 vs [ν_s(CO)], 1850 vs [ν_s(CO)].

X-ray crystallography: The X-ray data for the crystals of the compounds **4**, **7**, **9**, **10**, **11**, **12**, **13**, **14**·CH₂Cl₂, **15**, **16**·¹/₂Me₂CO and **18** were obtained at 150 K using an Oxford Cryostream low-temperature device on a Nonius KappaCCD diffractometer with Mo Kα radiation (λ = 0.71073 Å) and a graphite monochromator. Data reductions were performed with DENZO-SMN.^[34] The absorption was corrected by integration methods.^[35] Structures were solved by direct methods (Sir92)^[36] and refined by full-matrix least squares based on F² (SHELXL97).^[37] Hydrogen atoms were mostly localized on a difference Fourier map. However, to ensure uniformity of the treatment of the crystal, all hydrogen atoms were recalculated into idealized positions (riding model) and assigned temperature factors U_{iso}(H) = 1.2[U_{eq}(pivot atom)] or 1.5U_{eq} for the methyl moiety with C–H = 0.96, 0.97, and 0.93 Å for methyl, methylene, and hydrogen atoms in aromatic rings or the allyl moiety, respectively. Thermal ellipsoids of fluorine atoms of tetrafluoroborate anion in **11** were improved with standard ISOR instruction implemented in SHELXL97 software.^[37] In **10**, the same problem was solved by splitting of four fluorine atoms to two positions with nearly equal occupancy by using SAME, RIGU and EADP instructions in SHELXL-2013.^[38] There are residual electron maxima and small cavities within the unit cell probably originated from the disordered solvent (acetonitrile) in the structure of **15**. PLATON/SQUEZZE^[39] was used to correct the data for the presence of disordered solvent. A potential solvent volume of 306 Å³ was found. 78 electrons per unit cell worth of scattering were located in the void. The calculated stoichiometry of solvent was calculated to be three molecules of acetonitrile per unit cell which results in 66 electrons per unit cell. The same procedure was used for structure of **14** resulting in a potential solvent volume of 100 Å³ and 46 electrons. The calculated stoichiometry of solvent was calculated to be one molecule of dichloromethane per unit cell which results in 42 electrons per unit cell. Moreover, the fluorine atoms in disordered tetrafluoroborate anion were split into two positions with occupancy 7:3. CCDC 1486921–1486931 contain the supplementary crystallographic data for this paper. These data can be obtained free of charge from The Cambridge Crystallographic Data Centre.

Computational details: All calculations were performed with the GAUSSIAN 09 software package^[40] using the B3LYP gradient-corrected exchange–correlation functional^[41] in combination with the LanL2TZ basis set^[42] augmented with an f-polarization function^[43] for Mo and the standard 6-31G(d,p) basis set^[44] for the remaining elements. The geometry optimizations were carried out without symmetry constrains. Transition state optimizations were performed with synchronous transit-guided quasi-Newton method (STQN).^[45] Frequency calculations were performed to confirm the nature of minima and stationary points. One

imaginary frequency was observed for each transition state and none for minima. Each transition state was further confirmed by following the intrinsic reaction coordinate (IRC) on both sides.^[46] The solvent effects were considered in all energy calculations using polarizable continuum model (PCM).^[47] The free energy changes at 298.15 K were then calculated from equation: ΔG = ΔH – TΔS.

Acknowledgements

This work was supported by Ministry of Education of the Czech Republic (Project no. UPA SG360003). Access to computing and storage facilities owned by parties and projects contributing to the National Grid Infrastructure MetaCentrum, provided under the programme "Projects of Large Research, Development, and Innovations Infrastructures" (CESNET LM2015042), is greatly appreciated.

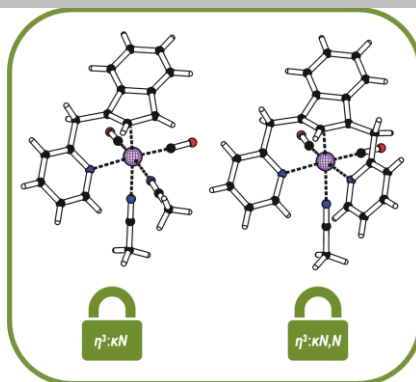
Keywords: hapticity • cyclopentadienyl • indenyl • molybdenum • intramolecular coordination

- [1] (a) T. J. Kealy, P. L. Pauson, *Nature* **1951**, *168*, 1039–1040; (b) E. O. Fischer, W. Pfab, *Z. Naturforsch. B* **1952**, *7*, 377–379; (c) S. A. Miller, J. A. Tebboth, J. F. Tremaine, *J. Chem. Soc.* **1952**, 632–635; (d) H. Werner, *Angew. Chem. Int. Ed.* **2012**, *51*, 6052–6058. (e) G. Wilkinson, M. Rosenblum, M. C. Whiting, R. B. Woodward, *J. Am. Chem. Soc.* **1952**, *74*, 2125–2126. (f) G. Wilkinson, *J. Am. Chem. Soc.* **1952**, *74*, 6146–6147.
- [2] (a) B. Topolinski, B. M. Schmidt, S. Higashibayashi, H. Sakurai, D. Lentz, *Dalton Trans.* **2013**, *42*, 13809–13812; (b) J. M. Speck, M. Korb, A. Schade, S. Spange, H. Lang, *Organometallics* **2015**, *34*, 3788–3798; (c) C. He, J. Wang, Z. Gu, *J. Org. Chem.* **2015**, *80*, 7865–7875; (d) W. Geng, C. Wang, J. Guang, W. Hao, W. X. Zhang, Z. Xi, *Chem. Eur. J.* **2013**, *19*, 8657–8664; (e) A. Donoli, A. Bisello, R. Cardena, M. Crisma, L. Orfan, S. Santi, *Organometallics* **2015**, *34*, 4451–4463; (f) A. Zirakzadeh, A. Herlein, M. A. Groß, K. Mereiter, Y. Wang, W. Weissensteiner, *Organometallics* **2015**, *34*, 3820–3832; (g) M. Roemer, K. Y. Kang, Y. K. Chung, D. Lentz, *Chem. Eur. J.* **2012**, *18*, 3371–3389; (h) Y. Yan, T. M. Deaton, J. Zhang, H. He, J. Hayat, P. Pageni, K. Matyjaszewski, C. Tang, *Macromolecules* **2015**, *48*, 1644–1650; (i) S. Ursillo, D. Can, H. W. P. N'Dongo, P. Schmutz, B. Spingler, R. Alberto, *Organometallics* **2014**, *33*, 6945–6952; (j) A. R. Petrov, K. Jess, M. Freytag, P. G. Jones, M. Tamm, *Organometallics* **2013**, *32*, 5946–5954.
- [3] (a) J. Schejbal, J. Honzík, J. Vinklár, M. Erben, Z. Růžičková, *Eur. J. Inorg. Chem.* **2014**, 5895–5907; (b) W. Y. Wang, N. N. Ma, S. L. Sun, Y. Q. Qiu, *Phys. Chem. Chem. Phys.* **2014**, *16*, 4900–4910; (c) X. Wang, D. Li, W. Deuther-Conrad, J. Lu, Y. Xie, B. Jia, M. Cui, J. Steinbach, P. Brust, B. Liu, H. Jia, *J. Med. Chem.* **2014**, *57*, 7113–7125; (d) H. Li, H. Zhang, Q. Zhang, Q. W. Zhang, D. H. Qu, *Org. Lett.* **2012**, *14*, 5900–5903; (e) Z. Liu, A. Habtemariam, A. M. Pizarro, S. A. Fletcher, A. Kisova, O. Vrana, L. Salassa, P. C. A. Buijinninx, G. J. Clarkson, V. Brabec, P. J. Sadler, *J. Med. Chem.* **2011**, *54*, 3011–3026; (f) G. Jaouen, A. Vessieres, S. Top, *Chem. Soc. Rev.* **2015**, *44*, 8802–8817; (g) Y. Yokota, Y. Mino, Y. Kanai, T. Utsunomiya, A. Imanishi, K. Fukui, *J. Phys. Chem. C* **2015**, *119*, 18467–18480; (h) A. Schmed, A. Straube, T. Grell, S. Jähnigen, E. Hey-Hawkins, *Dalton Trans.* **2015**, *44*, 18760–18768.
- [4] (a) B. Ye, N. Cramer, *Science* **2012**, *338*, 504–506; (b) B. Ye, N. Cramer, *J. Am. Chem. Soc.* **2013**, *135*, 636–639; (c) K. Sünkel, S. Weigand, A. Hoffmann, S. Blomeyer, C. G. Reuter, Y. V. Vishnevskiy, N. W. Mitzel, *J. Am. Chem. Soc.* **2015**, *137*, 126–129; (d) S. Harder, D. Naglav, C. Ruspici, C. Wickleder, M. Adlung, W. Hermes, M. Eul, R. Pöttgen, D. B. Rego, F. Poineau, K. R. Czerwinski, R. H. Herber, I. Nowik, *Chem. Eur. J.* **2013**, *19*, 12272–12280; (e) L. D. Field, C. M. Lindall, A. F. Masters, G. K. B. Clentsmith, *Coord. Chem. Rev.* **2011**, *255*, 1733–1790; (f) M. Erben, D. Veselý, J. Vinklár, J. Honzík, *J.*

- Mol. Catal. A: Chem.* **2012**, 353–354, 13–21; (g) S. Heinl, M. Scheer, *Chem. Sci.* **2014**, 5, 3221–3225; (h) T. Liu, X. Wang, C. Hoffmann, D. L. DuBois, M. R. Bullock, *Angew. Chem. Int. Ed.* **2014**, 53, 5300–5304; (i) M. Fang, E. S. Wiedner, W. G. Dougherty, W. S. Kassel, T. Liu, D. L. DuBois, M. R. Bullock, *Organometallics* **2014**, 33, 5820–5833; (j) A. Iordache, M. Oltean, A. Milet, F. Thomas, B. Baptiste, E. Saint-Aman, C. Bucher, *J. Am. Chem. Soc.* **2012**, 134, 2653–2671; (k) D. Patel, A. Wooles, A. D. Cornish, L. Steven, E. S. Davies, D. J. Evans, J. McMaster, W. Lewis, A. J. Blake, S. T. Liddle, *Dalton Trans.* **2015**, 44, 14159–14177.
- [5] A. J. Hart-Davis, R. J. Mawby, *J. Chem. Soc. A* **1969**, 2403–2407.
- [6] M. J. Calhorda, C. C. Romão, L. F. Veiros, *Chem. Eur. J.* **2002**, 8, 868–875.
- [7] (a) A. J. Hart-Davis, C. White, R. J. Mawby, *Inorg. Chim. Acta* **1970**, 4, 441–446; (b) D. J. Jones, R. J. Mawby, *Inorg. Chim. Acta* **1972**, 6, 157–160.
- [8] (a) C. A. Bradley, I. Keresztes, E. Lobkovsky, V. G. Young, P. J. Chirik, *J. Am. Chem. Soc.* **2004**, 126, 16937–16950; (b) L. F. Veiros, J. Honzík, C. C. Romão, M. J. Calhorda, *Inorg. Chim. Acta* **2010**, 363, 555–561.
- [9] L. F. Veiros, M. J. Calhorda, *Dalton Trans.* **2011**, 40, 11138–11146.
- [10] M. J. Calhorda, C. A. Gamelas, I. S. Gonçalves, E. Herdtweck, C. C. Romão, L. F. Veiros, *Organometallics* **1998**, 17, 2597–2611.
- [11] C. A. Gamelas, N. A. G. Bandeira, C. C. L. Pereira, M. J. Calhorda, E. Herdtweck, M. Machuqueiro, C. C. Romão, L. F. Veiros, *Dalton Trans.* **2011**, 10513–10525.
- [12] J. Lodinský, J. Vinklár, L. Dostál, Z. Růžicková, J. Honzík, *RSC Adv.* **2015**, 5, 27140–27153.
- [13] J. Honzík, J. Vinklár, M. Erben, J. Lodinský, L. Dostál, Z. Padělková, *Organometallics* **2013**, 32, 3502–3511.
- [14] C. C. Romão, *Appl. Organomet. Chem.* **2000**, 14, 539–548.
- [15] J. W. Faller, C. C. Chen, M. J. Mattina, A. Jakubowski, *J. Organomet. Chem.* **1973**, 52, 361–386.
- [16] (a) P. R. Mitchell, R. V. Parish, *J. Chem. Educ.* **1969**, 46, 811–814; (b) I. Langmuir, *Science* **1921**, 54, 59–67.
- [17] T. F. Wang, T. Y. Lee, J. W. Chou, C. W. Ong, *J. Organomet. Chem.* **1992**, 423, 31–38.
- [18] A. Avey, T. J. R. Weakley, D. R. Tyler, *J. Am. Chem. Soc.* **1993**, 115, 7706–7715.
- [19] O. Mrózek, L. Šebestová, J. Vinklár, M. Řezáčová, A. Eisner, Z. Růžicková, J. Honzík, *Eur. J. Inorg. Chem.* **2016**, 519–529.
- [20] (a) S. M. Bruno, A. C. Gomes, C. A. Gamelas, M. Abrantes, M. C. Oliveira, A. A. Valente, F. A. A. Paz, M. Pillinger, C. C. Romão, I. S. Gonçalves, *New J. Chem.* **2014**, 38, 3172–3180; (b) A. C. Gomes, C. A. Gamelas, J. A. Fernandes, F. A. A. Paz, P. Nunes, M. Pillinger, I. S. Gonçalves, C. C. Romão, M. Abrantes, *Eur. J. Inorg. Chem.* **2014**, 3681–3689; (c) J. Honzík, I. Honzík, J. Vinklár, Z. Růžicková, *J. Organomet. Chem.* **2014**, 772–773, 299–306.
- [21] (a) Y. Pan, W. Rong, Z. Jian, D. Cui, *Macromolecules* **2012**, 45, 1248–1253; (b) S. Wang, Y. Feng, L. Mao, E. Sheng, G. Yang, M. Xie, S. Wang, Y. Wei, Z. Huang, *J. Organomet. Chem.* **2006**, 691, 1265–1274; (c) C. Qian, H. Li, J. Sun, W. Nie, *J. Organomet. Chem.* **1999**, 585, 59–62.
- [22] (a) C. J. Wu, S. H. Lee, S. T. Yu, S. J. Na, H. Yun, B. Y. Lee, *Organometallics* **2008**, 27, 3907–3917; (b) Z. Ziniuk, I. Goldberg, M. Kol, *J. Organomet. Chem.* **1997**, 545–546, 441–446; (c) M. L. Buil, M. A. Esteruelas, A. M. López, A. C. Mateo, E. Onate, *Organometallics* **2007**, 26, 554–565.
- [23] L. F. Groux, D. Zargarian, *Organometallics* **2003**, 22, 3124–3133.
- [24] J. W. Faller, R. H. Crabtree, A. Habib, *Organometallics* **1985**, 4, 929–935.
- [25] J. R. Ascenso, I. S. Gonçalves, E. Herdtweck, C. C. Romão, *J. Organomet. Chem.* **1996**, 508, 169–181.
- [26] M. J. Calhorda, L. F. Veiros, *Coord. Chem. Rev.* **1999**, 185–186, 37–51.
- [27] J. Honzík, J. Vinklár, Z. Padělková, L. Šebestová, K. Foltánová, M. Řezáčová, *J. Organomet. Chem.* **2012**, 716, 258–268.
- [28] K. B. Wiberg, *Tetrahedron* **1968**, 24, 1083–1096.
- [29] W. L. F. Armarego, D. D. Perrin, *Purification of Laboratory Chemicals*, Butterworth-Heinemann, Oxford, **1996**.
- [30] G. Wilkinson, *Org. Synth., Coll. Vol* **1963**, 4, 473.
- [31] L. Meurling, *Acta Chem. Scand. B* **1974**, 28, 295–300.
- [32] P. W. Hickmott, S. Wood, P. Murray-Rust, *J. Chem. Soc., Perkin Trans. 1* **1985**, 2033–2038.
- [33] P. W. Causey, M. C. Baird, S. P. C. Cole, *Organometallics* **2004**, 23, 4486–4494.
- [34] Z. Otwinowski, W. Minor, *Methods Enzymol.* **1997**, 276, 307–326.
- [35] P. Coppens, *Crystallographic Computing* (Eds.: F. R. Ahmed, S. R. Hall, C. P. Huber), Munksgaard, Copenhagen, **1970**, pp. 255–270.
- [36] A. Altomare, G. Cascarano, C. Giacovazzo, A. Guagliardi, M. C. Burla, G. Polidori, M. Camalli, *J. Appl. Cryst.* **1994**, 27, 435–436.
- [37] G. M. Sheldrick, *SHELXL97*, University of Göttingen, Germany, **2008**.
- [38] G. M. Sheldrick, *Acta Cryst.* **2015**, C71, 3–8.
- [39] A. L. Speck, *Acta Cryst.* **2015**, C71, 9–18.
- [40] M. J. Frisch, G. W. Trucks, H. B. Schlegel, G. E. Scuseria, M. A. Robb, J. R. Cheeseman, G. Scalmani, V. Barone, B. Mennucci, G. A. Petersson, H. Nakatsuji, M. Caricato, X. Li, H. P. Hratchian, A. F. Izmaylov, J. Bloino, G. Zheng, J. L. Sonnenberg, M. Hada, M. Ehara, K. Toyota, R. Fukuda, J. Hasegawa, M. Ishida, T. Nakajima, Y. Honda, O. Kitao, H. Nakai, T. Vreven, J. Montgomery, J. A., J. E. Peralta, F. Ogliaro, M. Bearpark, J. J. Heyd, E. Brothers, K. N. Kudin, V. N. Staroverov, R. Kobayashi, J. Normand, K. Raghavachari, A. Rendell, J. C. Burant, S. S. Iyengar, J. Tomasi, M. Cossi, N. Rega, N. J. Millam, M. Klene, J. E. Knox, J. B. Cross, V. Bakken, C. Adamo, J. Jaramillo, R. Gomperts, R. E. Stratmann, O. Yazyev, A. J. Austin, R. Cammi, C. Pomelli, J. W. Ochterski, R. L. Martin, K. Morokuma, V. G. Zakrzewski, G. A. Voth, P. Salvador, J. J. Dannenberg, S. Dapprich, A. D. Daniels, Ö. Farkas, J. B. Foresman, J. V. Ortiz, J. Cioslowski, D. J. Fox, Gaussian, Inc., Wallingford CT, **2009**.
- [41] (a) A. D. Becke, *Phys. Rev. A* **1988**, 38, 3098–3100; (b) A. D. Becke, *J. Chem. Phys.* **1993**, 98, 5648–5652; (c) C. T. Lee, W. T. Yang, R. G. Parr, *Phys. Rev. B* **1988**, 37, 785–789; (d) B. Miehlich, A. Savin, H. Stoll, H. Preuss, *Chem. Phys. Lett.* **1989**, 157, 200–206.
- [42] (a) P. J. Hay, W. R. Wadt, *J. Chem. Phys.* **1985**, 82, 299–310; (b) L. E. Roy, P. J. Hay, R. L. Martin, *J. Chem. Theory Comput.* **2008**, 4, 1029–1031.
- [43] A. W. Ehlers, M. Böhme, S. Dapprich, A. Gobbi, A. Höllwarth, V. Jonas, K. F. Köhler, R. Stegmann, A. Veldkamp, G. Frenking, *Chem. Phys. Lett.* **1993**, 208, 111–114.
- [44] (a) W. J. Hehre, R. Ditchfield, J. A. Pople, *J. Chem. Phys.* **1972**, 56, 2257–2261; (b) P. C. Hariharan, J. A. Pople, *Theor. Chem. Acc.* **1973**, 28, 213–222.
- [45] (a) C. Peng, H. B. Schlegel, *Isr. J. Chem.* **1994**, 33, 449–454; (b) C. Peng, P. Y. Ayala, H. B. Schlegel, M. J. Frisch, *J. Comp. Chem.* **1996**, 17, 49–56.
- [46] (a) K. Fukui, *Acc. Chem. Res.* **1981**, 14, 363–368; (b) H. P. Hratchian, H. B. Schlegel, *J. Chem. Phys.* **2004**, 120, 9918–9924.
- [47] J. Tomasi, B. Mennucci, R. Cammi, *Chem. Rev.* **2005**, 105, 2999–3093.

FULL PAPER

The unusual example of a low hapticity lock is reported on the indenyl compounds with intramolecularly coordinated pyridine arms. The combined experimental and theoretical study reveals a high stability of $\eta^3:\kappa N$ - and $\eta^3:\kappa N,N$ -coordination compounds toward η^3 to η^5 haptotropic rearrangement.



O. Mrózek, J. Vinklárek, Z. Růžicková,
J. Honzík*

Page No. – Page No.

**Indenyl compounds with
constrained hapticity: the effect of
strong intramolecular coordination.**